MOLECULAR GENETICS OF END STAGE KIDNEY AND ASSOCIATED RENAL CELL TUMOURS

PhD Thesis

Anetta Nagy, MD

Head of Doctoral School: Gabor L. Kovacs, MD, PhD, DSc

Head of Doctoral Program: Istvan Wittmann, MD, PhD, DSc

Supervisor: Gyula Kovacs, MD, PhD, DSc, FRCPath

Medical School, University of Pecs, Pecs

2016

CONTENTS

1. INTRODUCTION

1.1 End-stage renal disease and its significance

Chronic renal disease (CRD) is a public health problem all over the world with a considerable socioeconomic burden (1-3). Kidney failure is the last (fifth), most severe stage of CRD, defined as a GFR below 15 mL per minute per 1.73 m^2 body surface area (4). The term 'end-stage renal disease' (ESRD) reflects a clinical condition in which there has been an irreversible loss of endogenous renal function, of a degree sufficient to render the patient permanently dependent upon renal replacement therapy (RRT) - dialysis or kidney transplantation - in order to avoid life-threatening uremia.

There is an increasing incidence and prevalence of the ESRD population. Annual growth rate of ESRD patient is estimated to increase with 6-7% for recent years and exceeded the annual growth rate of 1.2% of general world population (5). Based on estimations of United States Renal Data System, the number of patients treated with RRT for kidney failure was 287.000 in 1995, nearly 500.000 in 2005 and is projected to increase to more than 750.000 by 2020 (1).

The rising prevalence of ESRD is the consequence of the continuing increase of diabetes mellitus type 2 and hypertension worldwide. The growing number of patients with ESRD is influenced by several factors (e.g. improved overall survival of patients at higher risk for ESRD, more liberal entry into and better survival on RRT), of which the global epidemic of type 2 diabetes mellitus and the ageing of the general population are especially emphasized (6). The number of ESRD patients on long-term dialysis (usually more then ten years) is growing as well.

Although, less than 2% of the CRD patients progresses to ESRD, the associated high - particularly cardiovascular - morbidity and mortality rates and high medical expenditures make it important from a public health perspective. In Europe, dialysis alone accounts for about 2% of health-care budgets with less than 0.1% of the population needing treatment. ESRD is a substantial burden on health care systems, particularly in developing countries with other health care priorities (7).

1.2. Morphological features of ESRD kidneys

Despite the advancements achieved in general nephrology, the final outcome of a significant number of CRD cases is still ESRD. The common histopathologic features of the characteristically shrunken end-stage kidneys displaying tubular atrophy, interstitial inflammation and fibrosis, severe arterial, arteriolar and glomerular sclerosis result directly or indirectly from loss of functional and structural integrity. By the time of terminal uremia the kidneys may have much the same morphological appearance irrespectively of primary renal disease which excludes the exact recognition of original disease, particularly in kidneys of patients on chronic dialysis (8, 9).

The RRT prolongs and improves the life of ESRD patients, especially when their disease is limited to the kidney and results in a novel type of renal histology that have rarely been seen before. The progressive structural changes, i.e. considerable fibrosis and intimal arterial thickening (Figure 1A) and widespraed deposition of calcium, calcium oxalate or calcium phosphat crystals (Figure 1C) have already been mentioned by Heptinstall (8). The unique morphologic changes were described in detail by McManus and Hughson in a series of papers about 30 years ago (10-13).

They have reported microscopic cellular nodules of smooth muscle cell proliferation arising around arterial and arteriolar necrosis as well as the increase in arterial intimal thickness due the increased growth of endothelial and smooth muscle cells (Figure 1D). The diverse froms of tubules of end-stage kidneys were classified into „classic" atrophic tubules, tubules showing „thyroidization" (Figure 1B), „endocrine" tubules and „super" tubules. The latter ones are enlarged and dilated and lined with hyperplastic/hypertrophic epithelium (Figure 1E) (14). Fibrotic renal interstitium may harbour isolated single cells or loosely organized small groups of cells (clusters) with epithelial characteristics which are not surrounded by a visible basement membran at the light microscopic level. In spite of atrophic, scarred structures, end stage kidney shows a remarkable proliferative activity, especially in the epithelium of „classic" atrophic and „super" tubules. The unusual high proliferative activity has also been observed in papillary proliferation of cells lining dialted tubules or small microscopic cysts (Figure 1F).

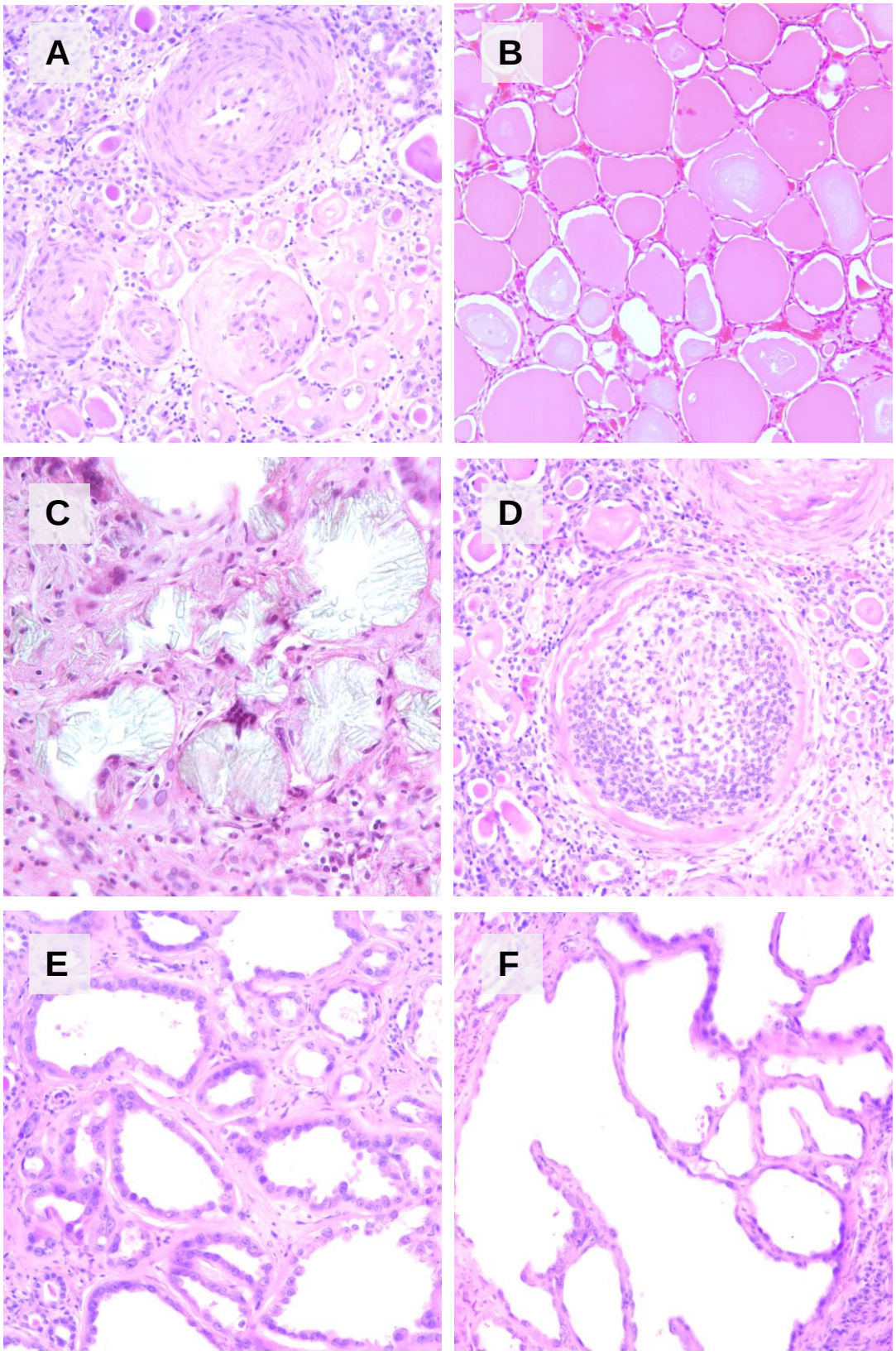

Figure 1. Characteristic histological picture of morphological changes in kidneys with ESRD.

1.3. Acquired cystic renal disease (ACRD)

The cystic changes in failing kidneys was already noted in the 19th century but it was given no any attention until 1977, when Dunnill, Millard and Oliver described the bilateral diffuse cystic changes of sclerotic end-stage kidneys after long-term intermittent maintenance haemodialysis (9). They pointed out its possible complications, i.e. haemorrhage and formation of benign and malignant renal tumors. ACRD is a bilateral disorder characterized by the development of multiple renal cysts in uremic patients with initial cyst-unrelated renal disease (15). There is no uniform diagnostic criteria in the literature, the expected number of detectable cysts ranges from one to five or more than five in radiologic (16,17) and a cystic alteration in 25% to 40% of the renal parenchyma for tissue-based studies (18). Although the continuous progression of cystic changes renders these criteria somewhat arbitrary, the diagnosis of ACRD accepted generally requires the presence of more than 3 cysts or more than 25% of tissue involvement in each kidney and the exclusion of hereditary cystic kidney diseases (19). A cross section of a kidney with ACRD is shown in Figure 2A. Note the high number of smaller of larger cysts, the rest of fibrotic renal parenchyma and also a circumscribed necrotic tumour on the left slide of the picture.

The multiple, bilateral thinwalled cysts disorganize the architecture of renal parenchyma. They predominate in the cortex, but occur also in the renal medulla or at corticomedullary junction (9, 20). The cysts contain tipically clear or straw-colored fluid into which bleeding is not uncommon (19). Deposition of oxalate crystals is tipical of ACRD and manifests often in the walls or cavities of the cysts or within the tubules or interstitium (9, 12, 21).

The cysts are lined by simple monolayer eosinophilic epithelium (Figure 2 B), sometimes higher hobnail-like cells (Figure 2C). The proliferative cysts display in most cases a papillary growth of eosinophilic cells (Figure 2D). In some cysts proliferation of large eosinophilic cells with vacuolated cytoplasma may be observed, which corresponds to precursor lesions of ESRD-associated eosinophilic tumours (Figure 2E).

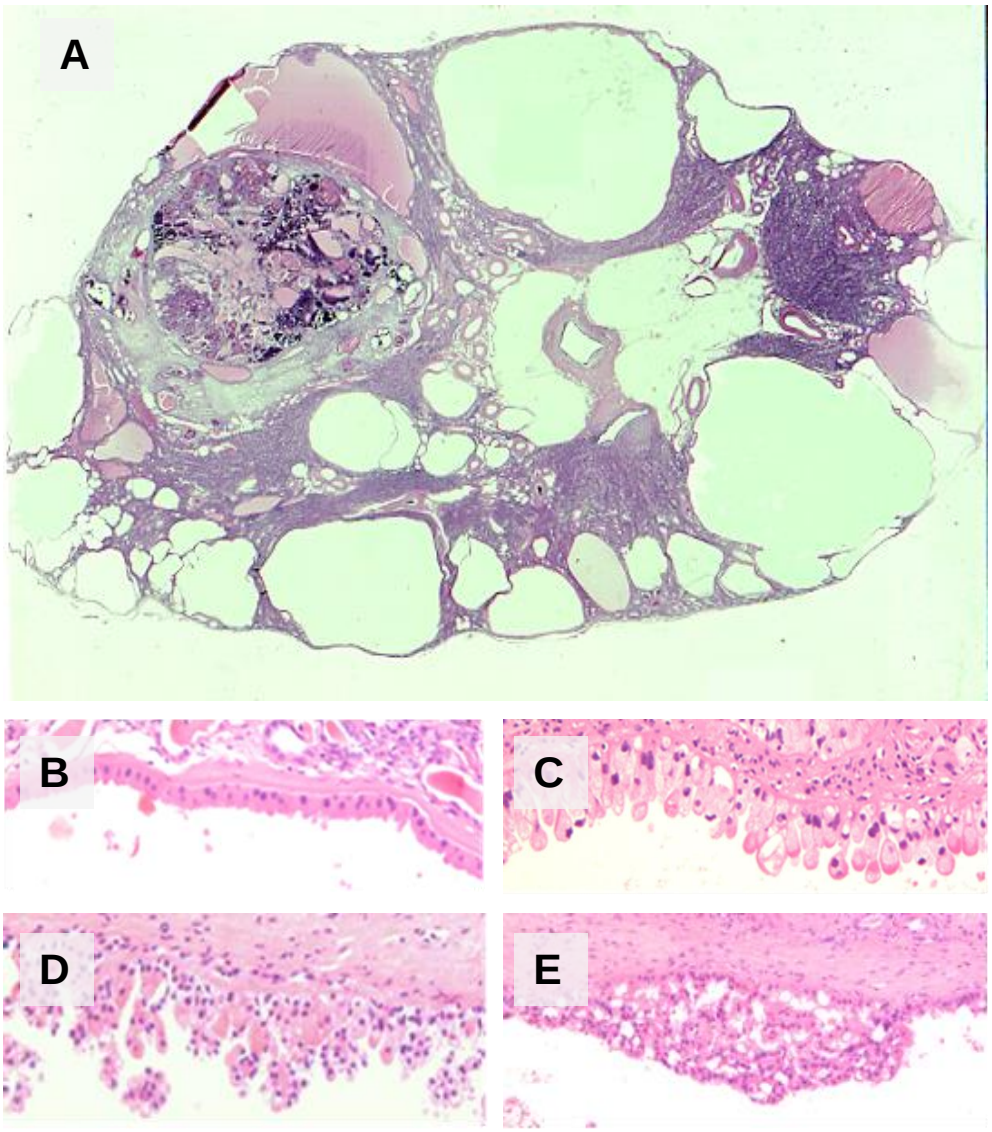

Figure 2. Gross section of ACRD and morphology of associated cysts.

Microdissection studies have demonstrated continuity between cysts and tubules suggesting that cysts begin as outpouching of any of the tubular segments and develop into cysts through continuous proliferation of tubular cells (19). Although cysts in ACRD may originate from different segments of nephron, lectin and immunhistochemical studies suggested that the vast majority of cysts are derived from proximal tubules (19, 21). The similarity of marker distribution in the „super" tubuli and cysts in ACRD also favours the assumption that cysts may originate from these tubules (14).

The occurrence of ACRD and the extent of cystic degeneration correlate consistently with the duration of dialysis confirming its progressive nature (22, 23).

The occurrence is reported from 30% to 95% in various populations of dialyisis patients studied, presenting an overall rate of around 45% and reaching virtually 100% after 10 years of dialysis. The high occurrence of ACRD in those undergoing long-term dialysis suggest that its development is a natural consequence and the final fate of end-stage kidneys resulting from various diffuse renal parenchymal diseases. Although ACRD is usually clinically silent, its possible complications are urolithiasis, renal colic associated with stone passage or blood clots, cyst rupture, cyst infection or erythrocytosis, but more frequently haemorrhage ranging from intracystic bleeding, micro- or macrohaematuria to subcapsular or retroperitoneal haematoma. However, the cardinal and clinically most significant complication of cystic transformation is the development of RCTs.

1.4. Renal cell tumors in ESRD/ACRD

Renal cell tumors develop in patients with ESRD/ACRD at higher frequency than in the general population and RCT also occur frequently in native kidneys of renal transplant recipients (24-27). Of interest, RCTs develop 5-7 times more frequently in males, which is higher male predominance than the occurrence of ESRD/ACRD itself (28). Approximately 10% of ESRD/ACRD-associated RCTs are bilateral (10%) and around 30% of tumours are multifocal (29). However, the vast majority of tumours are less then 3 cm in diameter and remain asymptomatic.

The natural history, genetics and histological variation of RCTs as well as the differentiation between benign and malignant tumors developing in the general population have already been established (30,31). Nearly 50% of the neoplasm in ESRD/ACRD display papillary or tubulo-papillary growth pattern, whereas papillary RCT make up only 10% of cases in the general population (32). Recently, tumours with unusual histological pattern and DNA alteration occurring in ESRD/ACRD have been published (33-37). A unique type of ESRD/ACRD associated tumor is charactrized by solid/papillary/cystic growth of large eosinophilic cells having large cytoplasmic vacuoles (Figure 3A) (33). Moreover, intratumoral calcium oxalate deposition in tumours composed of large eosinophilic cells with occasional cytoplasmic vacuolization (Figure 3B) and tumours with cribriform growth pattern or “clear cell papillary” RCTs (Figure 3C, D) habe been described (34, 38).

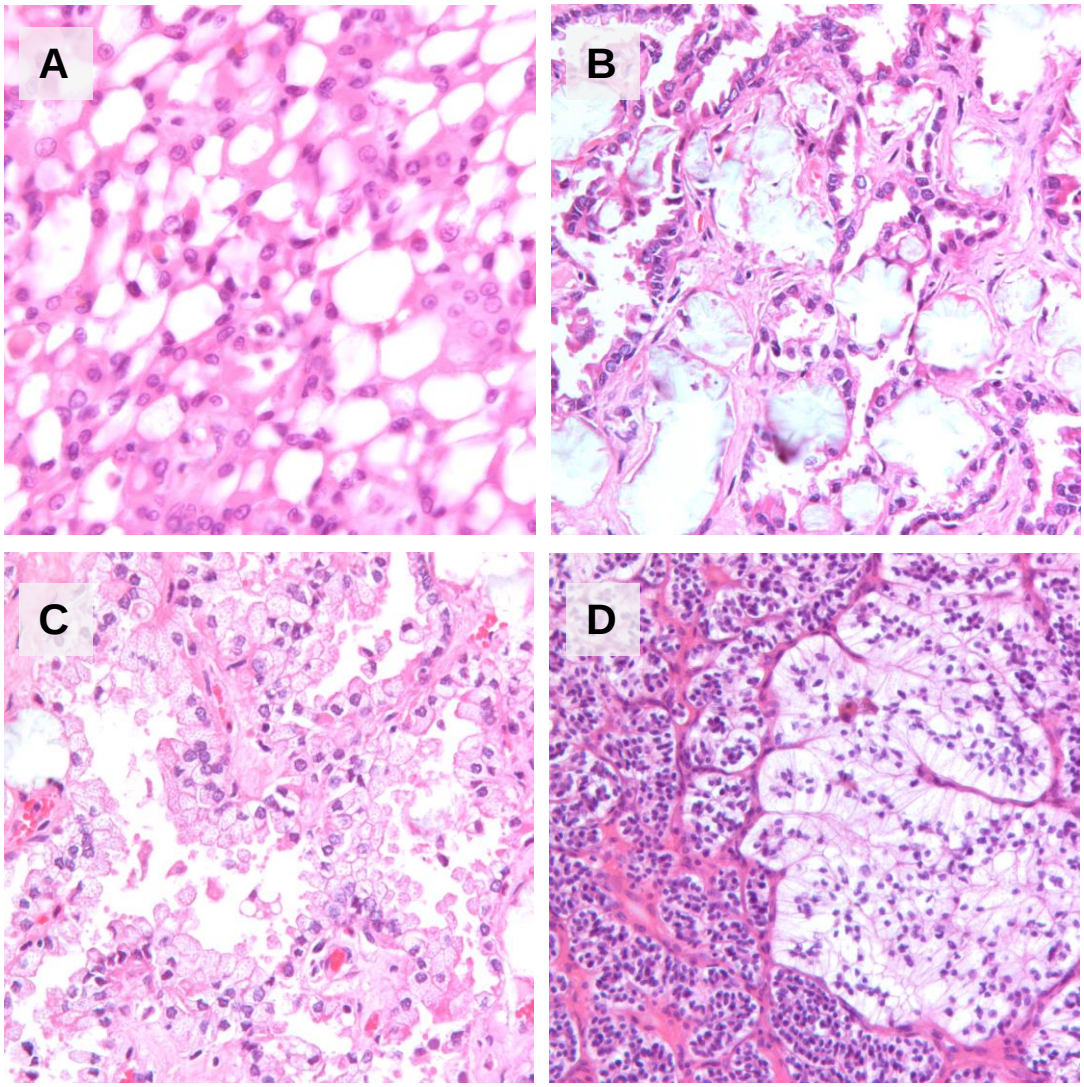

Figure 3. Histological variation of ESRD/ACRD associated renal cell tumours.

In addition to unique phenotypic features the genetic constitution of RCTs arising from end-stage kidneys may also differ from those known to be characteristic for sporadic cases. Based on molecular genetic analysis, the genetic alterations in some ESRD/ACRD tumours correspond with those characteristical in RCTs occuring in the general population but others just fail to present – partly or totally - the most typical chromosomal changes, may have distinct genetic changes or do not show any alterations (33-37). In the case of unusual tumor morphology, the diagnosis and biological behavior of some of the ESRD/ACRD tumors remain uncertain even after molecular characterization. Although further studies are necessary, the available data

suggest that the initial developmental step for RCC associated with ESRD/ACRD might be slightly different from those occuring in the general population (39).

1.5. Pathogenesis of ESRD/ACRD and tumours

In spite of histochemical and molecular genetic studies, the biology of proliferating parenchymal and interstitial cells as well as the molecular mechanisms leading to formation of multiple cysts, remodelling the kidney parenchyma and development of unique type of tumours remains unknown. The loss of kidney function in chronic renal diseases is associated with structural changes of nephrons and chronic inflammation in scarring stroma. An increased rate of cell division has been found in cells of atrophic tubuli as well as in stromal cells suggesting that end stage kidneys is not a quescient organ (14).

There are many factors suggested to be instrumental in cystic remodeling and tumorigenesis. Uremic syndrome actually affecting all organ system is attributed to the progressive retention of a large number of potentially toxic compounds not excreted into the urine. Increased genomic damage has been shown in uremic patients such as elevated rate of sister chromatic exchange or formation of micronuclei (40-42). The efficiency of DNA repair is decreased to about 60% in uraemic patients but remained nearly normal in patients having a maintanance dialysis (43).

Toxic effects in the uraemic state or during maintenance dialysis may have remarkable pathological consequences on mitochondria (44-46). The deletion of a 4977 bp segment known as the most common large-scale deletion of mtDNA in various human tissues have been described to occur in the skeletal muscle, in hair follicles and in peripheral blood cells of ESRD patients with a significantly higher incidence than in those of age-matched controls (47, 48). Mitochondria are considered to be the main source of intracellular oxidative stress by generation of ROS with incomplete reduction of oxygen at several sites on the electron transfer chain (49). The mtDNA is more vulnerable to genotoxic agents and has a considerable higher mutational rate than that of nuclear DNA. Its vulnerability is increased presumably due to the the lack of proofreading mechanisms during mtDNA replication, the low capacity of repair mechanisms as well as the absence of protective histones. Damage to mtDNA can accumulate and mutations may cause

alterations in the components of the respiratory chain with decreased enzymatic activities resulting in increased generation and accumulation of intracellular ROS probably due to enhanced electron leakage from their defective electron transport chains (50-52). Elevated levels of ROS could further impair important proteins, interfere with metabolic pathways, contributes to nuclear genome damage and cancer initiation (51).

Specific renal cell growth factor, mitogenic substances, accumulation of epidermal growth factor or activation of signal transduction molecules (e.g. cyclic AMP) in cystic fluid are implicated in the proliferation of renal epithelial cells (53-56). Increased level of growth factors and their receptors such as hepatocyte growth factor (*HGF*) and its receptor c-met (*MET*)and insulin-like growth factor-1 (*IGF-1*) has also been suggested to be involved in remodeling of end stage kidneys (57, 58).) Other suggested the role of hypoxia-inducible protein 2 (*HIG-2*) and hypoxia-inducible factor-1α (*HIF-1α*) in ESRD/ACRD biology (59). Altered expression of proto-oncogens or amplification of *c-erb* B-2, activation of c-*jun* and hyper methylation of connexin 32 have been published (60-62). The role of cytokins such as interleukin-6 (*IL-6*), interleukin-8 (*IL-8*) and vascular endothelial growth factor (*VEGF*) accumulating in acquired cysts was also proposed (63). It was suggested that possible mechanical effect of calcium oxalate monohydrate crystals deposited in renal epithelial cells may induce proliferation by altering their gene expression. (64)

The aforementioned studies have analysed only one or two genes or one kind of genomic alteration, but no systematic analysis of the molecular microenvironment of ESRD/ACRD kidneys have been carried out.

1.6. Aim of the study

Based on the dynamic structural changes in ESRD/ACRD and because the phenotype and genotype of RCTs developing in ESRD/ACRD may differ from the those occurring in the general population, an alternative pathway of tumor development reflecting the special microenvironment in ESRD/ACRD has been proposed (39).

Based on this background, the following issues have been raised:

1. Are genotoxic effects of uremic milieu in ESRD patients responsible for genetic instability and subsequently to development of tumours?
2. Which genes and mechanisms are involved in hyperplastic-cystic remodeling and/or strong predisposition for tumorous process of end-stage kidneys?
3. Does this remodeling resembles a disorganized embryonal development or regeneration of kidneys, or corresponds to a novel type of disease?
4. Is there a common factor relevant to both the high risk of RCC and the increased overall cancer risk in ESRD?

In an attempt to clarify these problems, my work aimed to:

1. Sequence the entire mitochondrial genome in renal parenchymal cells from patients with ESRD/ACRD and in RCCs arising in end-stage kidneys.
2. Sequence the *VHL* and *MET* genes and analyse the genomic changes in ESRD/ACRD associated tumours.
3. Establish the global gene expression profile in ESRD/ACRD kidneys and compare to that of embryonal and adult normal kidneys and distinct types of renal cell tumors by using Affymetrix oligonucleotide microarray.
4. Improve the expression of the selected genes in a panel of cDNA samples of the aforementioned tissues by quantitative RT-PCR.
5. Determine the cellular localisation of the encoded proteins in embryonal, adult and ESRD/ACRD kidneys as well as in distinct types of renal cell tumours by immunohistochemistry.

2. PATIENTS AND METHODS

2.1. Sample collection and histological diagnosis

Fresh kidney specimens and nine renal cell tumours from patients with ESRD/ACRD as well as specimens of a large number of adult kidneys and distinct types of renal cell tumours were obtained from the Urological Departments in Germany (Heidelberg, Bad-Hersfeld), United Kingdom (Oxford Radcliffe Hospital), Hungary (Budapest), Austria (Linz) and Slovenia (Ljubljana). None of the patients underwent transplantation prior to nephrectomy.

Fresh tissue samples were processed for analysis immediately after nephrectomy. Beside a part of tumour tissue used for cell culture and cytogenetic analysis, one part of fresh renal parenchymal tissue and of tumour tissue was snap-frozen in liquid nitrogen and stored at −80°C for DNA, RNA and protein analysis. The rest of tumour tissue and the remaining nephrectomy specimen were fixed in 4% buffered formaldehyde for histological examination.

Paraffin embedded samples from 21 ESRD/ACRD cases were also available. Altogether, in 12 of the 21 cases the entire kidney was sectioned and processed for histological analysis. Fetal kidneys from 13, 18 and 19 weeks of pregnancy were obtained after legal abortus at the Department of Gynecology, University of Pecs, Hungary (Dr. Béla Veszprémi). The collection and use of all tissue samples for this study was approved by the Ethics Committee of the University of Heidelberg and University of Pecs, Hungary.

In end-stage kidneys, ACRD was diagnosed when the secondary cystic changes replaced at least 40% of the kidney parenchyma. The histopathological diagnosis of tumours arising in ESRD and non-ESRD kidneys was established according to the Heidelberg Classification (31) and to Tickoo et al. (34).

2.2. Mitochondrial and genomic DNA analysis

Isolation of high molecular weight genomic DNA. Genomic DNA from normal parenchymal and tumour tissues of end-stage kidneys was extracted by phenol-

chlorophorm according to standard procedures. First, frozen kidney tissues were placed in a plastic Petri dish, covered with TE9 buffer and allowed to thaw. The tumour cells were then carefully scraped off or pushed out to separate them from stromal tissue under an inverted microscope by a pathologist (Professor Kovacs) experienced in this technique. Stromal components were discarded. By this way, contamination of DNA by normal cells was reduced to less than 5%.

Tumour cells were resuspended in 5 ml of TE9 buffer and mixed with 250 µL of 20% SDS and 100 µL of 20 mg/mL proteinase K. The samples were incubated at 55°C for at least 3 h or until complete digestion. Then, equal to previously used TE9 buffer volume of phenol was added and mixed gently for 5 min. Phases were separated by centrifugation for 10 min at 3000 rpm at room temperature. The upper, aqueous layer (wihout any phenol rest) was collected, transferred to a new tube, supplemented by the equal volume of chloroform, mixed gently for 5 min and centrifuged like before. This step with chloroform was repeated. DNA was precipitated with 2.5 volume of 100% ethanol (according to the aqueous layer), air-dried and dissolved in $TE_{10/1}$ buffer. Control DNA was extracted from corresponding kidney parenchymal specimens by the same method.

The DNA quantification was based on absorbance at 260 nm (A_{260}) and the quality of DNA was estimated from the absorbance ratios at 260 and 280 nm ($A_{260/280}$) as well as at 260 and 230 nm ($A_{260/230}$) by NanoDrop®ND-1000 spectrophotometer measurements. DNA integrity was controlled on a 1.2% (w/v) agarose gel by electrophoresis in TAE buffer (see also in 2.2.3.9). The size of the DNA was estimated by comparison with marker run alongside with the samples and electrophoresis was documented by the AlphaDigiDoc® RT Gel Documentation System. Samples were stored at 4°C.

Primers and amplification of mtDNA. We have designed 24 pairs of primers that amplify overlapping fragments of approximately 900 bp of the complete 16 569 bp of mitochondrial DNA (mtDNA). Primer sequences are available upon request. The forward and reverse primers were tailed at their 5' ends with the sequences of universal primers UP21 (5`-TGT AAA ACG ACG GCC AGT-3`) for forward and RP29 (5`-CAG GAA ACA GCT ATG ACC–3`) for reverse one, to allow direct sequencing of the PCR products. PCR amplification was performed in 20 µL reaction volume with 20 ng of genomic DNA, 2.0 mM $MgCl_2$, 0.5 µM each primer,

200 µM each dNTP, and 3.0 U of Taq polymerase. Amplification programme consisted of an initial denaturation of 2 min at 94°C followed by three cycles with 30 s at 95°C, 30 s at 65°C, and 1 min at 72°C, and 25 two-step cycles with 20 s at 95°C and 1 min at 72°C with a terminal elongation of 5 min at 72°C. The PCR products were analysed for appropriate size by electrophoresis on a 1.5% agarose gel. Then 1 µl of the PCR product was sequenced with universal primers UP21 labelled with IRD700 dye and RP29 labelled with IRD800 dye by using the SequiTherm EXCEL™ II Long-Read DNA Sequencing Kit according to the manufacturer's instructions. The PCR programme was as follows: initial denaturation for 5 min at 95°C and 29 cycles with 15 s at 95°C, 30 s at 57°C, and 1 min at 70°C. Amplifications and sequencing reactions were carried out in a PTC-200 DNA Engine® Cycler machine.

Polyacrylamide gel electrophoresis (PAGE). For electrophoresis, a 66 cm polyacrylamide gel was poured with 0.2 mm spacers between the glass plates. Beside 7 M urea, 1 x TBE and distilled water, 3.75% of acrylamide (from a 40% stock solution PAGE-PLUS™ Concentrate), 0.66% (v/v) 10% APS and 0.066% (v/v) TEMED was used to prepare a denaturing gel matrix, which was applied through a filter on the top of the syringe. After gel polimerization, samples of sequencing reaction were denatured for 3 min at 80°C and 1 µl of them was loaded onto the gel. The electrophoresis was performed on a LI-COR Long Read IR^2 4200 Automated DNA Sequencer working with dual-laser system detecting IRD700 and IRD800 dyes at the same time. Running conditions were as follows: 3000 V of voltage, 30 mA of current, 75 W of power at 45°C temperature using 0.8 x TBE running buffer diluted from 10 x TBE. The raw data were collected and analysed with the e-Seq™ Software (v. 2.0), which creates two independent image files with information from the 700 and 800 channel disclosing nucleotide sequences of forward and reverse DNA strands, respectively.

Sequencing of samples requiring cloning. Direct sequencing of some samples gave illegible sequences from the poly(C) tract of the D-loop region onwards, requiring these samples to clone into vector. PCR fragments were ligated using the pGEM®-T and pGEM®-T Easy Vector Systems with the 2x Rapid Ligation Buffer and T4 DNA Ligase, then transformed into XL1-Blue Supercompetent Cells in accordance with the manufacturer`s recommendations. Positive clones characterized by blue/white

screening were checked by colony PCR reactions performed in 10 µL volume with 1.5 mM $MgCl_2$, 0.8 µM each standard primer (T7: 5'-TAA-TAC-GAC-TCA-CTA-TAG-GG-3`; SP6: 5'-ATT-TAG-GTG-ACA-CTA-TAG-AA-3'), 200 µM each dNTP, and 0.25 U of Taq polymerase. The conditions of amplification were an initial denaturation of 3 min at 94°C followed by 35 cycles with 30 sec at 94°C, 30 sec at 55°C, and 1 min at 72°C, and a terminal elongation of 5 min at 72°C. PCR products were visualised by agarose gel electrophoresis on 1.2% (w/v) gel. Then plasmid DNA from the overnight cultures of seven colonies of each sample was purificated with the Concert Rapid Plasmid System Kit following the manufacturer`s protocols. After measuring of plazmid DNA concentrations (in ng/µL) by spectrophotometry, the optimal volumen of samples (in µL) for the sequencing reactions was calculated based on the calculated amount of DNA samples (in ng) equal to 250 fmol. The calculation was performed from the next starting formula:

$$\frac{\text{Plazmid DNA concentration (ng/µL) x 1515}}{\text{Number of nucleotids (bp): vector+insert}} = \text{..... fmol/µL DNA}$$

Sequencing reaction with the appropriate IRD700- and IRD800-labelled sequencing primers, PAGE and evaluation were performed as described above.

2.3 Sequence analysis of *VHL* and *MET*

We have sequenced the three exons of the *VHL* gene from genomic DNA of four RCTs obtained from kidneys of two ESRD patients with ACKD, including two conventional RCCs and two ACKD-associated RCTs. First, the samples were amplified with nested primer pairs encompassing the coding region of exon 1, exon 2 or exon 3 of the VHL gene, respectively, in 10 µL reaction volume with 50 ng of genomic DNA, 1.5 mM $MgCl_2$, 200 nM each primer, 50 µM each dNTP, and 0.5 U Taq polymerase. In the case of exon 1, Q-Solution was also added because of the amplicon`s high GC (guanosin and cytosine) content. The amplification programme consisted of an initial denaturation of 2 min at 95°C followed by 35 cycles with 30 sec denaturation at 94°C, 30 sec annealing at 55°C (exon 1) or at 60°C (exon 2; exon 3), and 45 sec extension at 72°C, then a final elongation of 5 min at 72°C.

For the second round of amplification the primer pairs were tailed at their 5´-ends with the sequences of universal primers UP21 (5`-TGT AAA ACG ACG GCC AGT-3`) for forward and RP29 (5`-CAG GAA ACA GCT ATG ACC–3`) for reverse one, to allow direct sequencing of the PCR products. One µL of the amplified products was reamplified in 20 µL reaction volume with 1.5 mM $MgCl_2$, 500 nM each primer, 200 µM each dNTP, 1 U Taq polymerase, and again with Q-Solution in the case of exon 1. PCR conditions were as follows: 2 min of initial denaturation at 95°C followed by 4 cycles with 30 sec at 94°C, 30 sec at 65°C and 1 min at 72°C, then 13 two-step cycles with 20 sec at 95°C and 1 min at 70°C. PCR product of amplification and reamplification reactions was analysed for size and quality by electrophoresis on a 2 % agarose gel. Sequences of the nested and tailed primers are listed in Table 3.

Table 1. Nested and tailed primer sequences of the *VHL* gene

Exon	***Sequence***
Exon 1-F	5'-AGC GCG TTC CAT CCT CTA C-3'
-R	5'-CGT GCT ATC GTC CCT GCT-3'
Exon 2-F	5'-GTG GCT CTT TAA CAA CCT TTG C-3'
-R	5'-CCT GTA CTT ACC ACA ACA ACC TTA TC-3'
Exon 3-F	5'-TTC CTT GTA CTG AGA CCC TAG T-3'
-R	5'-AGC TGA GAT GAA ACA GTG TAA GT-3'
Exon 1-F	5'-C*TG TAA AAC GAC GGC CAG T*CG TTC CAT CCT CTA CCG-
-R	5'-C*CA GGA AAC AGC TAT GAC C*AT CGT CCC TGC TGG GTC-
Exon 2-F	5'-C*TG TAA AAC GAC GGC CAG T*AA CAA CCT TTG CTT GTC-
-R	5'-C*CA GGA AAC AGC TAT GAC C*AC AAC AAC CTT ATC TTT-
Exon 3-F	5'-C*TG TAA AAC GAC GGC CAG T*CT GAG ACC CTA GTC TGC-
-R	5'-C*CA GGA AAC AGC TAT GAC C*AA ACA GTG TAA GTT TCA-

Then 1 µl of the reamplification product was sequenced using 2 µM universal primers UP21 labelled with IRD700 and RP29 labelled with IRD800 dye by applying the Thermo Sequenase™ Fluorescent Labelled Primer Cycle Sequencing Kit with 7-Deaza dGTP according to the manufacturer's instructions. The PCR programme was as follows: initial denaturation for 2 min at 95°C, then 30 cycles with 20 s at 95°C, 30 s at 57°C, and 1 min at 70°C. Amplifications and sequencing reactions were carried out in a PTC-200 DNA Engine® Cycler machine.

After this procedure, 6 µL of stop/loading buffer was added to the altogether 6 µL of reaction volume. The electrophoresis was performed on a LI-COR Long Read IR^2 4200 Automated DNA Sequencer working with dual-laser system detecting IRD700 and IRD800 dyes at the same time with some differences as follows: because of the shorter sequencing products a 41 cm long, 0.25 mm thick 6% denaturing gel was used with appropriate running conditions, i.e. 1500 V of voltage, 25 mA of current, 36.5 W of power at 46°C temperature. The read sequences were analysed by eSeq2.0 software and were compared to the wild-type sequence (J02958) to identify mutation. (GenBank ID: NM_000551.2).

Exons 16, 17, 18 and 19 of the proteine kinase domain of the *MET* gene were prepared for sequencing as described earlier (65). The amplified *MET* exons were directly sequenced with an IR800 and IR700-labeled sequencing primer set using the Thermosequenase cycle sequencing kit (Amersham Pharmacia) following the manufacturers advices. The labeled products of the sequencing reaction were analyzed in both directions simultaneously on the dual laser scanner LICOR Long Readir 4200 sequencing machine using the BaseImagIR software package as described above. The read sequences were compared to the wild-type sequence to identify mutation.

2.4. CGH (Comparative Genomic Hybridization)

We have analysed ESRD/ACRD associated tumours for genomic alterations by applying the Agilent Oligonucleotide Array-Based CGH. High molecular weight DNA was isolated from short term cell-culture, whereas a pool of sex matched DNA isolated by phenol-chloroform method from five normal parenchymal kidneys was used as a reference for array CGH. DNA was treated with proteinase K and RNAse A, and further purified on the columns using the DNeasy Blood and Tissue Kit according to the manufacturer's procedure. Its quality and quantity was assessed by NanoDrop®ND-1000 spectrophotometer measurements.

For array CGH analysis, 500 ng of sample and reference DNA was fragmented and chemically labelled with ULS™ Cy3 and Cy5 dyes, respectively, according to the Agilent Oligonucleotide Array-Based CGH for Genomic DNA Analysis user guide (v. 3.1). Further hybridization to 4x44K array (AMADID 014950), washing

and scanning procedures were carried out at the Genomics Core Facility, EMBL (Heidelberg, Germany) according to the manufacturers' protocol. Data were further extracted from the scanned microarray image (.tif), filtered and normalized by the Agilent Feature Extraction software (v. 9.5), and analyzed using the Agilent CGH Analytics software (shot time free trial v. 3.4). Statistically significant regions of aberration in a given sample were determined by the ADM-2 algorithm according to the sensitivity threshold at 6.0 and a moving average window of 1 Mb. A copy number gain was defined as a $\log_2$ ratio >0.3 and a copy number loss was defined as a $\log_2$ ratio <-0. 3.

2.5. Gene expression analysis

2.5.1 Global gene expression analysis using Affymetrix platform

Isolation of RNA with TRIzol® reagent. For expression analysis, 100 mg of frozen kidney and tumor tissues were homogenized by ULTRA-TURRAX™ in 1 mL TRIzol® Reagent and total ribonucleid acid (RNA) was isolated according to the manufacturer's instructions. In brief, after 5 min incubation at room temperature, 200 µL of chloroform pro each 1 mL of TRIzol® Reagent was added. Tubes were vigorously shaken by hand for 15 sec, incubated at room temperature for 3 min and centrifuged for 15 min at 12.000 x g at 4°C. The aqueous, upper phase was transferred into a fresh tube. RNA was precipitated with 0.5 mL isopropyl alcohol by incubation for 10 min at room temperature followed by centrifugation for 10 min at 12.000 x g at 4°C. Pellet was dissolved in 4M lithium chloride at room temperature and centrifuged again for 5 min at 15.000 x g at 4°C. Thereafter the pellet was washed twice with 1 mL of 75% ethanol, in between mixed and centrifuged for 5 min at 7.500 x g at 4°C, air-dried and resuspended in DEPC-treated water by vortexing and briefly heating at 50°C. RNA was dissolved in 1xSSC. The concentration and quality of total RNA was assessed by spectrophotometry at 260 nm (A_{260}) and absorbance ratios at 260 and 280 nm ($A_{260/280}$) in a NanoDrop®ND-1000 spectrophotometer. RNA integrity was checked on a 1.2% (w/v) agarose gel in

formaldehyde denaturing conditions and electrophoresis was documented by the AlphaDigiDoc® RT Gel Documentation System. Samples were stored at -70°C.

For microarray analysis, total RNA was isolated from six ESRD/ACRD kidney samples, normal kidneys and distinct types of RCTs (Table 4). Total RNA of ESRD/ACRD and embryonal and adult kidneys samples as well as from distinct types of renal cell tumours including embryonal ones was purified by using the RNeasy Mini Kit according to the manufacturer`s protocol in order to obtain high-quality RNA. The quality was assessed by spectrophotometry and denaturing agarose gel electrophoresis as described above. We have pooled RNA of best quality from adult kidneys, Wilms' tumours, papillary RCC and conventional RCC with and without progression of the disease as well as from renal oncocytoma and chromophobe RCC for Affymetrix array analysis.

The cRNA synthesis and array hybridization were performed by the Affymetrix Screening Service at the German Resource Center for Genome Research in Berlin (RZPD, http://www.rzpd.de). Each sample of high quality cRNA was hybridized once using the Affymetrix Human Genome U133 A and B array set. One signal per gene was obtained using standard Affymetrix procedures (http://www.affymetrix.com/estore/browse/products.jsp?productId=131536&categoryId=35760). The scanned image files were converted by the GeneChip® Operating Software (GCOS, Affymetrix) and the raw data obtained are available at the Gene Expression Omnibus repository under accession number GSE6280 (GEO, http://www.ncbi.nih.gov/geo/).

The intensity data (44,928 probesets) were normalized using default settings in MicroArray Suite software (MAS v. 5.1, Affymetrix) and further processed using Microsoft Excel. The gene expression was correlated to those of pooled normal adult kidneys with number 3 and 16 in Table 2. The value in the pooled normal adult kidney samples was used as a baseline reference and relative expression values in pooled tumour samples were calculated. The transcripts that showed an adjusted signal log2 ratio above 1 or less than 1 in tumour samples were considered to be upregulated or downregulated, respectively.

Table 2. Samples used for Affymetrix-array analysis.

number	***Sample***
1.	Normal kidney, 12 weeks old fetus
2.	Normal kidney, 21 weeks old fetus
3.	Normal adult kidney, pooled
4.	Wilms' tumor, pooled
5.	Clear cell sarcoma of the kidney
6.	Papillary renal cell tumor, pooled,
7.	Papillary renal cell carcinoma,
8.	Conventional RCC, pooled, pT1,G1
9.	Conventional RCC, pooled, pT3,G3
12.	Chromophobe RCC, pooled
13.	Renal oncocytoma, pooled
14.	Normal kidney, 13 weeks old fetus
15.	Normal kidney, 20 weeks old fetus
16.	Normal adult kidney pooled
17.	ESRD kidney, HD94
18.	ACKD kidney HD105
19.	ACKD kidney, HD123
20.	ACKD kidney, HD195
21.	ACKD kidney, HD 209
22.	ESRD kidney, HD217

The analysis of expression profiles was performed on a whole dataset without any prior feature selection. We used correspondence analysis to explore the relationships between the samples in a low-dimensional projection of expression data (66). The computation of principal components and data visualization were performed using the microarray data analysis tool TIGR Multiexperiment Viewer (TMeV, http://www.tm4.org/mev/). Unsupervised hierarchical clustering was further done with the same software using Euclidian correlation as measurements of similarity and average linkage.

For selection of diagnostic markers it is essential to minimize the overlap in their expression between two groups of samples. The commonly used variability-based methods (like T-test or FDR) do not test the overlap of the samples. The more so, genes with minor fold differences between groups of samples, even despite of their possible high statistical significance, would have less practical value as markers

and should not be selected. Therefore, the differentially expressed genes were identified using only quantitative fold-change criteria and qualitative metrics such as Presence/Absence and Increase/Decrease calls provided with MAS v. 5.1 algorithmus. Genes showing a signal log ratio over 2 in ESRD samples and under 0 in nearly all other samples with corresponding detection and change call, i.e. specifically up-regulated in ESRD and down-regulated in other type of tissues, were selected for qRT-PCR. In addition, genes showing an increased expression in ESRD/ACRD samples and one type of RCTs were also selected for RT-PCR. Significance analysis of microarrays (SAM) with all available number of permutations and fold-change 2.0 was performed to estimate statistical significance of the manually selected probesets as transcripts associated with ESRD/ACRD and ESRD/ACRD/papillary RCC (http://www-stat.stanford.edu-tibs/SAM).

To define functionally related genes among those specifically expressed in ESRD/ACRD kidneys and also in distinct types of renal cell tumours we applied the web-based DAVID Gene Functional Classification Tool (67). (http://david.abcc.ncifcrf.gov/gene2gene.jsp)

2.5.2. Reverse transcription polymerase chain reaction (RT-PCR)

Reverse transcription. In reverse transcription (first-strand cDNA synthesis) reactions, total RNA was transcribed with SuperScript™ II Reverse Transcriptase Kit and 3` one-base-anchored oligo-dT_{23} primers in 25 µl final reaction volume. In brief, 2 µg of RNA supplemented with DEPC-water up to a volume of 12 µL, 2 µL of 50µM oligo-dT_{23} and 2 µL of 10 mM dNTP mix were incubated for 5 minutes at 65°C, than cooled down on ice. Thereafter 5 µL of 5 x reverse transcription buffer, 2 µL of 0.1M DTT and 1 µL of 40U/µL RNase inhibitor (RNaseOUT™) were added and mixed. After 2 minutes incubation at 42°C, 1 µL of SuperScript™ II Reverse Transcriptase were also mixed. Reverse transcription reaction was carried out by incubation for 60 minutes at 42°C, then a second step for 30 minutes at 50°C. To obtain 1:4 concentration of cDNA, 75 µL of DEPC-treated water was added. After making 20 µL aliquots, samples were stored at -20°C.

Primer design for polymerase chain reaction (PCR). Sequences of the selected Affymetrix probes were obtained through the NetAffx™ Analysis Center

(http://www.affymetrix.com/analysis/index.affx). Primer pairs for the represented human genes and ESTs were constituted by the help of the Primer3 primer design software (http://frodo.wi.mit.edu/) with a contribution of NCBI Reference Sequences (RefSeq) from National Center for Biotechnology Information (www.ncbi.nlm.nih.gov) and Human BLAT Search (http://genome.brc.mcw.edu/cgi-bin/hgBlat) in order to obtain information about gene structure models, exon-exon junctions. If possible primers were designed in protein coding regions resulting in amplicons to cover an exon-exon junction. The next optimal parameters were observed: melting temperatures (T_m) of 60±3°C, primer lengths of 19-24 nucleotides, guanine-cytosine (GC) content of 38-56% and PCR amplicon length of 120-350 bp. To check primer specificity, the sequences were blasted against the nucleotide collection sequences using NCBI BLAST algorithm (http://www.ncbi.nlm.nih.gov/BLAST) with standard parameters. Primers were synthetised by MWG Biotech AG (http://www.mwg-biotech.com, http://www.eurofinsdna.com). Primer sequences and the annealing temperatures used in PCR conditions are available upon request.

Quantitative RT-PCR (QRT-PCR). For the expression analysis of the selected human genes and ESTs, a representing fragment of their cDNAs was amplified and the amount of the arising amplicons was monitored by performing qRT-PCRs in real time. As templates, a series of 1:8 diluted cDNAs originating from 2 normal foetus kidneys (13 and 19 weeks old), 5 normal adult kidney, 8 ESRD/ACKD kidney, 5 conventional RCCs, 5 papillary RCTs, 5 chromophobe RCCs and 5 renal oncocytomas were used (Table 2). Two µL of the diluted cDNA was amplified with 1 µM of each forward and reverse primer and 5 µL of the Platinum™ SYBR™ Green qPCR SuperMix UDG Kit in 10 µL final volume. Real-time PCRs were performed in optical 96-well plates using a DNA Engine Opticon™ Real-Time System. After a 2 min incubation at 50°C and an initial denaturation at 95°C for 2 min, the cycling parameters were 40 cycles of 95°C for 20 sec, 56-60°C (different optimal annealing temperature by primer pairs) for 30 sec and 72°C for 30 sec, then an additional 5 min elongation at 72°C. Samples were parallel amplified with the gene specific and the reference (houskeeping) gene (ACTB, i.e. β-actin: 5'-ATG GAT GAT GAT ATC GCC GCG-3' as forward and 5'-GTC CAT CAC GAT GCC AGT GGT AC-3' as reverse one) primers.

QRT-PCR assays were analysed with the Opticon Monitor Software package (v. 1.4). Specificity of the PCR products was verified by analysis of melting curves generated at the end of the cycles. For relative quantification, standard curves were performed from a 5-step dilution series (1:5:5:5:5) of pooled cDNA for both gene specific and reference gene reactions. After aligning quantitation curve, the software determined automatically the copy numbers reflecting the measure of gene expression. For calculation of relative expression levels, the representing numerical values of the gene specific expression were divided by that of the reference gene expression and the quotient was multiplied with 1000. All reactions were carried out in duplicates and the results were averaged.

Agarose gel electrophoresis in native conditions. In order to analyse and visualise PCR products or to control the quality and integrity of nucleid acids after isolation procedure, agarose gel electrophoresis was performed. The agarose concentration of a gel ranged from 0.8% to 2.5% mostly according to the expected size of nucleid acid fragments. To prepare a gel, agarose was melted in 1 x TAE or 1 x TBE buffer, then it run in the same buffer. Samples were mixed in appropriate proportions with loading buffer containing a dye and loaded on a gel by pipetting. The electrophoresis was carried out in electrophoresis chambers at 80-100 V until the full separation of the size marker loaded simultaneously with the samples. After electrophoresis, gels were post-stained in a 5µg/mL aquosus solution of ethidium bromide (EtBr) and shortly rinsed. (In the case of gels for RNA samples EtBr was added to the RNA loading buffer at a final concentration of 10µg/ml.) Samples in the gels were visualized by UV light. Recording the images with an enclosed camera, electrophoresis was documented by the AlphaDigiDoc® RT Gel Documentation System. The size of the products was estimated by comparison with the ladder.

2.6. Immunohistochemistry (IHC)

Tissue micro array (TMA) construction. In order to be able to analyse large number of tumour samples from ESRD/ACRD kidneys and from the general population we used TMA. TMAs were constructed from original formalin-fixed, paraffin-embedded material of ESRD/ACRD associated tumours as well as from Wilms' tumours, conventional, papillary and chromophobe RCCs and renal oncocytomas from the

general population. H&E stained slides from each paraffin donor block were analysed morphologically in order to select the representative areas per case. After marking the areas of interest, core biopsies of 0.6 mm in diameter were obtained with a precision instrument. We used a Manual Tissue Arrayer 1 for this purpose. The histomorphological selection and construction the TMAs was made by a pathologist experienced in this technique (Professor Kovacs). (Figure 4)

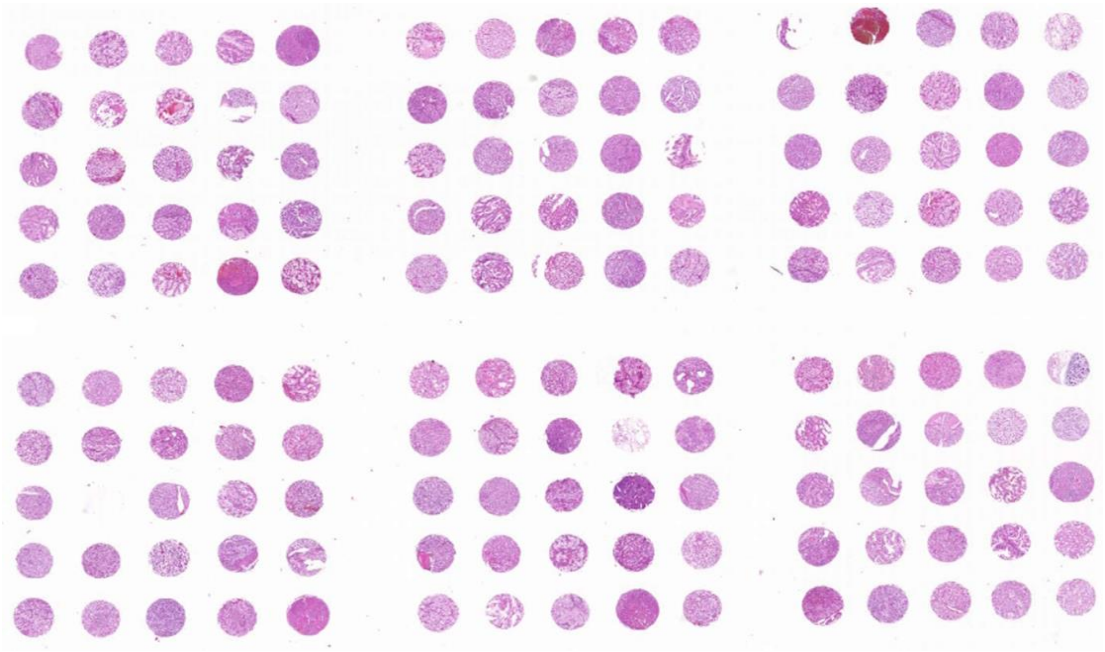

Figure 4. TMA containing six blocks of samples each with 25 tumour biopsy including fetal and adult normal kidneys to mark the TMAs and for controlling the quality of immunohistochemical staining.

Immunohistochemistry. Tissue sections from original formalin-fixed, paraffin-embedded archival tissue blocks containing fetal, adult and ESRD/ACRD kidneys as well as TMAs including one with ESRD/ACRD associated tumours, one with papillary RCTs and another one with conventional RCCs were analysed by immunohistochemistry.

After deparaffinisation and rehydration, the slides were treated in antigen unmasking solution of pH 9.0 and pH 6.0, respectively, in 2100-Retriever (Pick-Cell Laboratories, Amsterdam, Netherlands). After blocking the endogen peroxidase activity and nonspecific binding sites the slides were incubated overnight at 4C with primary antiserum listed in Table 3 at the indicated dilution. HRP conjugated anti-

rabbit and mouse secondary antibody (MACH4 Universal HRP-Polymer, Biocare Medical, Concord, USA) was then applied for 30 minutes and bound antibody was visualized with AEC (amino-ethyl-carbazol) or DAB plus (diaminobenzidine) chromogen solution (DAKO, Glostrup, Denmark). The sections were counterstained with Mayer's Hematoxylin (DAKO) and covered either with Ultramount or Pertex.

Table 3. Short characterisation of antibodies used in the gene expression analysis of ESRD/ACRD and tumours

Protein	Antibody	Type	Host	Supplier	Dilution
CSF2	PA1-84972	polyclonal	rabbit	Thermo Fisher	1:100
SCEL*	SC4	polyclonal	rabbit	Dr. H. P. Baden	1:300
GPR87	ab13945	polyclonal	rabbit	Abcam	1:100
CXCL8	AHC0881	polyclonal	rabbit	Thermo Fisher	1:100
CXCR2	#GTX71887	polyclonal	rabbit	Acris Antibodies	1:200
SAA1	ab655	monoclonal	mouse	Abcam	1:100
LBP	HPA 1508	polyclonal	rabbit	Atlas Antibodies	1:250
KRT7	#SP5355P	polyclonal	rabbit	Acris Antibodies	1:200
KRT19	#10954-1-AP	polyclonal	rabbit	ProteinTech	1:50

*The SC4 (anti-SCEL) antibody was kindly provided by Dr. H. P. Baden of the Massachusetts General Hospital/Harvard Medical School, Boston, MA, USA.

3. RESULTS

3.1. Data of ESRD/ACRD and renal cell tumours

Table 4. Pertinent clinical and histological data of ESRD/ACRD tumours

Tumour samples	*Patient age /gender*	*Renal disease*	*Size of kidney (cm)*	*Size of tumor (cm)*	*Histological diagnosis*
94A	76/M	ESRD/NS	9.5 x 6 x 3	0.8	cRCC
94B				0.2	pRCT
94C				0.3	pRCT
105	71/F	ACRD/?	12 x 6.5 x 5	4.0	RO
123A	77/M	ACRD/GN	15 x 8 x 7	3.1	ACRD-T
123B				2.6	cRCC
123C				2.2	ccpRCC
137	61/M	ESRD/NS	6.5x3.0x3.0	3.0	cRCC
173 L	68/M	ESRD/GN	5.5x3.0x1.5	2.5	chRCC-like
173 R			5.5x3.0x2.0	1.5	chRCC-like
192	49/M	ACRD/NS	10 x 5.5 x 3	3.5	cRCC
195	43/M	ACRD/?	9 x 5 x 4	3.0	cRCC
203 A	54/M	ESRD/?	7x3.5x2.5	4.1	pRCT
203 E				0.3	pRCT
209	49/M	ACRD/GN	9.5x5.5x4	3.2	ACRD-T
217	71/M	ESRD/?	6.5x3.5x3	2.8	cRCC
1926	33/M	ACRD/?	10x5x4	3.5	pRCT

Abbreviations: NS: nephrosclerosis; ?: unknown; GN: glomerulonephritis; cRCC: conventional RCC; pRCT: papillary RCT; RO: renal oncocytoma; ACRD-T: ACRD associated large eosinophilic cells with cytoplasmic vacuoles; ccpRCC: clear cell papillary RCC; chRCC-like: similar morphology to chRCC.

Pertinent clinical and histological data of ESRD tumours are listed in Table 4. In our collection of ESRD/ACRD associated tumours the smallest one measured 0.2 cm whereas the largest 4.1 cm. Small tumours or tumour-like lesions of microscopic size and also tumours in cyst are listed below in Table 5.

3.2. Morphology of ESRD/ACRD kidney

The morphology of ESRD as well as of ACRD kidneys correspond to that was described by McManus and Hudgson (10-13) and in the Introduction. In short fashion, ESRD kidneys showed a diffuse hyalinisation of glomeruli, tubular basemment and small or larger arteries. In several slides a strong proliferation of smooth muscle cells and endothelial cells obliterating the lumen occurred. Nearly all ESRD and also ACRD kidneys displayed large areas of „thyroidisation" composed of dilated tubules filled with eosinophilic fluid. Especially in the cortical areas dilated tubuli or larger cyst lined with flattened or hobnail cells were noticed.

ACRD kidneys are characterized by several cysts of different sizes and lined by different types of epithelium (see Figure 2). Some of them are filled with eosinophilic protein-containing fluid others seem to be emplty in paraffin embedded material. The vast majority of cysts are lined by a single layer of epithelium composed of flat or small cuboideal cells and large columnar epithelium in some cysts. ACRD kidneys displayed frequently atypical proliferativ cysts, which are possible precursor lesions for ACRD-associated tumours.

3.3. Morphology of microscopic lesions and tumours

Working up 12 entire kidneys obtained from patients with ESRD/ACRD in 393 paraffin blocks revealed 143 smaller or larger cysts, 26 proliferative cysts (including 10 with large eosinophyil cells displaying large cytoplasmic vacuoles, marked by star), 65 small papillary precursor lesions of small or medium sized cells, 42 precursor lesions with chromophobe RCC-like pattern, 24 small solid lesions with large eosinophyil cells containing large vacuoles. The large cysts of macroscopic size are not counted in this evaluation. The number of cysts and precursor lesions are shown in Table 5.

Table 5. Type and number of precursor lesions in ESRD/ACRD

Tumour samples	*Nr. of blocks*	*cyst*	*p-cyst*	*conv*	*pap*	*ch-like*	*l-eos*	*ccpap*
94	27	11	3	0	**21**	2	1	0
105	21	13	2	0	5	0	0	0
123	95	18	4*	0	**13**	0	**4**	1
137	32	3	0	**3**	2	0	0	0
173R	28	14	2	0	2	**19**	0	0
173L	24	7	0	0	1	**21**	0	0
192	23	6	0	**4**	0	0	0	0
195	29	38	12	**5**	2	0	0	0
203	25	11	2	1	5	0	0	0
209	40	12	6*	0	1	0	**19**	0
217	27	2	3	**4**	1	0	0	0
1926	22	8	2	0	**12**	0	0	0

Abbreviations. p-cyst: proliferative cyst; conv: conventional-like lesion; pap: papillary lesion; ch-like: chromophobe-like lesion; l-eos: large eosinophilic cells with vacuoles; ccpap: clear cell papillary lesion. The dominant type of precursor lesion is marked in bold.

We found a strong correlation between the number and type of precursor lesions of microscopic size and tumours in ESRD/ACRD kidneys. For example, the kidney (1926) of an ACRD patient contains 12 small papillary lesions of small “blue cell” (Figure 5A) and the small adenomas and the clinically detected tumour display similar cellular pattern (Figure 5B). In two kidneys (173R and 173L) of patient with ESRD the overwhelming majority of the precursor lesions (19 and 21, respectively) showed small nests of large “clear” cells and small nuclei (Figure 5C). All tumours repeated the same histology indicating their common origin (Figure 5D). In the ACRD kidney (209) each of the 6 proliferative cysts was lined by proliferative vacuolized eosinophilic epithel (Figure 5E) and each solid lesion displayed the same pattern (Figure 5F).

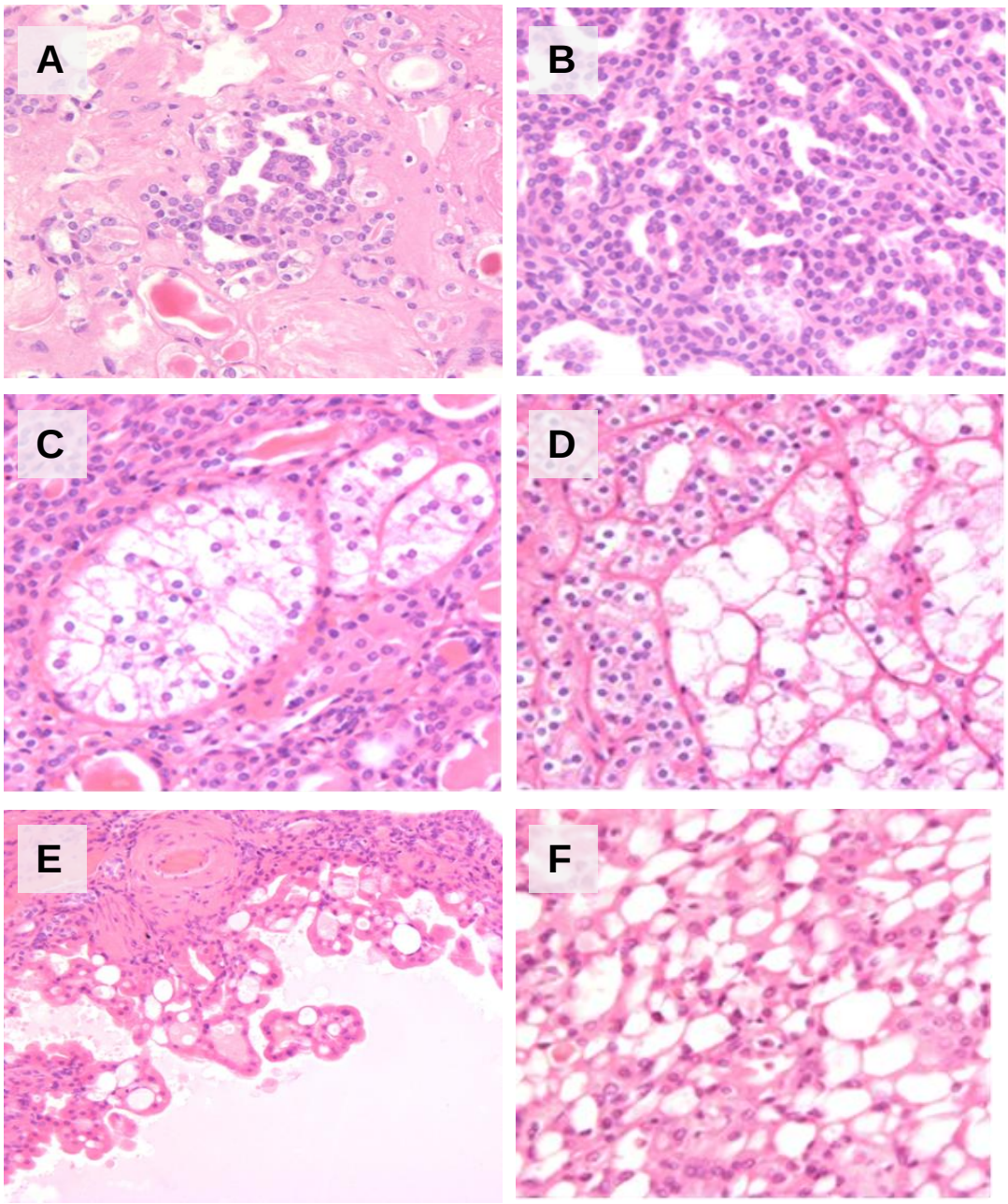

Figure 5. Precursor lesions and corresponding tumours of similar histology in ESRD/ACRD kidneys.

As it was shown in Table 2 and Table 3, the papillary precursor lesions and also tumours occurs in higher number as it is expected on the basis of their occurrance in the general population. Every second tumour was diagnosed as a conventional RCC, which represent around 80% of tumours in the general population. We detected several tumours of unusual morphology, which have never been seen before.

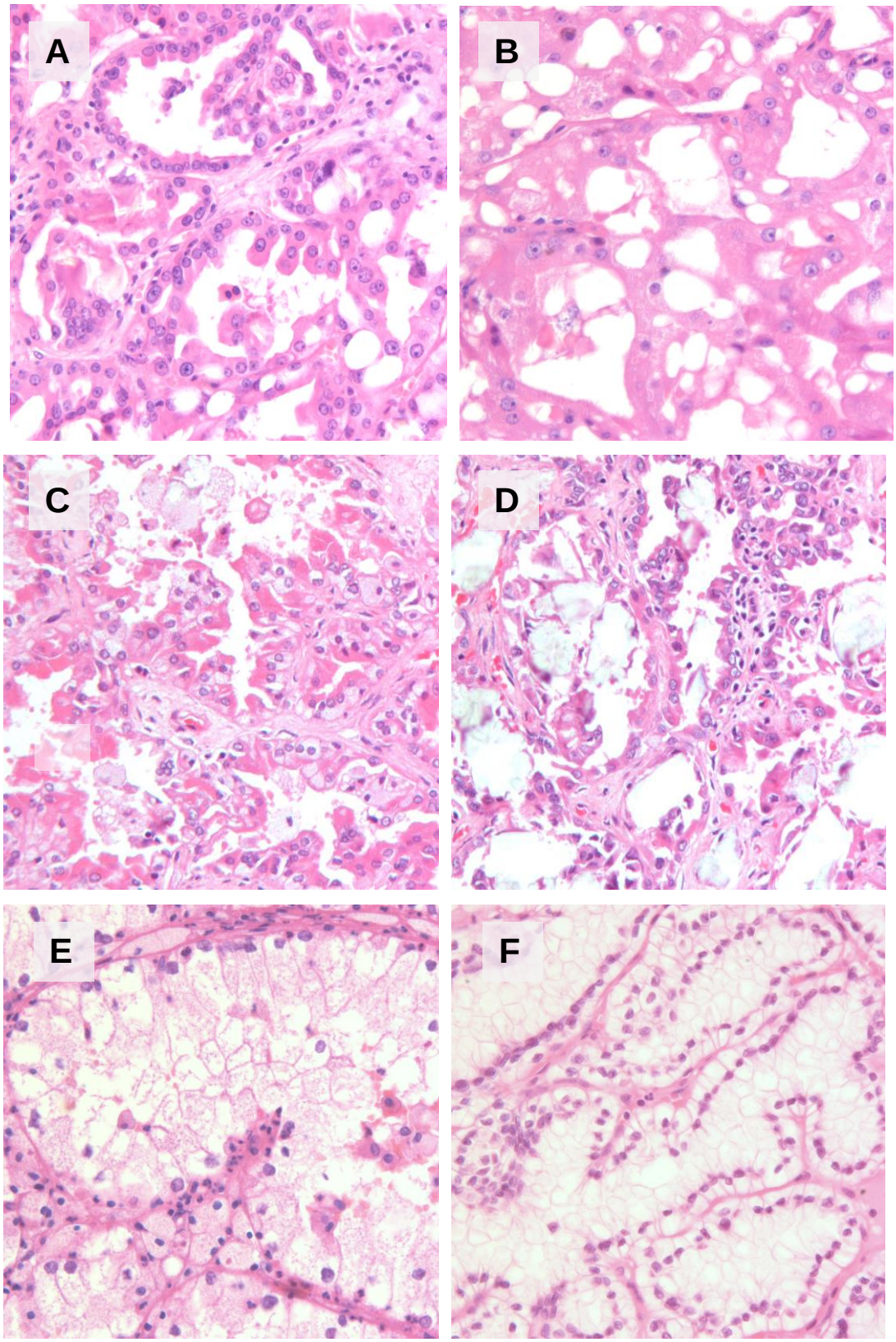

Figure 6. Unique morphology of ESRD/ACRD associated tumours.

Some of the papillary RCT (Figure 6A) undergone a profound morphological alteration into large ACRD associated tumour composed of large eosinophylic cells displaying cytoplamic vacuoles (Figure 6B). However, this type of tumour may develop de novo from proliferating cysts or small precursor lesions (see Figure 5E, F). Several papillary RCTs may exhibit large eosinophylic cells intermingled with clear cell like structures (Figure 6C). Some tumours in ESRD/ACRD kidneys contain large oxalate crystals either in the cytoplasm or in stroma (Figure 6D). The so called clear cell papillary RCC, which occurs rarely in the general population is characterised by papillary growth of large clear cells and sometimes foamy cell infiltration in the papillary stalks (Figure 6E). In rare cases the cell nuclei are lined at the surface of tumour cells displaying an unusual histological picture (Figure 6F). The latter one may also occur in rare cases in RCCs of the general population. In summary, not only the precursor lesions but also the tumours differed from those are known in the general population.

3.4. Mitochondrial DNA alterations in ESRD/ACRD kidneys and tumours

New sequence variants identified in the mitochondrial genome. The mtDNA sequences of both renal parenchymal cells and renal cell tumours were compared with those of the Mitomap database (http://www.mitomap.org). Sequence variants detected in both normal and tumour DNA were classified as polymorphisms. We found 94 mtDNA polymorphisms (4–27 per individual) in the kidneys of the six patients. Thirty-eight sequence variants occurred in the non-coding mtDNA control region, 12 in the rRNAs, four in tRNAs, and 40 polymorphisms in the polypeptide coding regions. Nearly half of the polymorphisms (44 of 94) were A to G substitutions. Nearly all of the polymorphic variants occurred in homoplasmic form (100% variants), but some of them were in heteroplasmic form, making up approximately 50–75% of the mtDNA. Only 34 of the 69 different sequence variants occurred in the protein coding region and of these, 19 (56%) resulted in alteration of the amino acid sequences. All but 20 polymorphisms have already been recorded in the Mitomap database. The new polymorphisms detected are listed in Table 6.

Table 6. New mtDNA polymorphisms detected in ESRD patients

Patient ID	*Location (nt)*	*Nuclotid change*	*Amino acid change*	*Gene (symbol)*
123	263	A → C	NA	NCR (MTOHR)
94;105;192;195;209	264	C → G	NA	NCR (MTOHR)
105	722	C → T	NA	MT-RNR1
192	1721	C → T	NA	MT-RNR2
123	4790	A → T	No change	MT-ND2
105	5042	A → G	No change	MT-ND2
209	5618	T → C	NA	MT-TA
195	6371	C →T	No change	MT-CO1
192	7768	A → G	No change	MT-CO2
105	8343	A → G	NA	MT-TK
195	8705	T → C	Met → Thr	MT-ATP6
209	8723	G → A	Arg → Gln	MT-ATP6
209	8812	A → G	Thr → Ala	MT-ATP6
123	12354	T → C	No change	MT-ND5
192	12634	A → G	Ile → Val	MT-ND5
105	12972	A → G	No change	MT-ND5
105	13434	A → G	No change	MT-ND5
192	13630	A → G	Thr → Ala	MT-ND5
195	14470	T → C	No change	MT-ND6
123	15892	T → C	NA	MT-TT

Abbreviations: NA: not applicable; NCR: non-coding region; MTOHR: mitochondrially encoded heavy strand origin of replication; MT-RNR1: mitochondrially encoded 12S RNA; MT-RNR2: mitochondrially encoded 16S RNA: MT-ND2 / MT-ND5 / MT-ND6: mitochondrially encoded NADH dehydrogenase 2 / 5 / 6; MT-TA / MT-TK / MT-TT: mitochondrially encoded tRNA alanine / lysine / threonine; MT-CO1 / MT-CO2: mitochondrially encoded cytochrome c oxidase I / II; MT-ATP6: mitochondrially encoded ATP synthase 6.

Alteration in the D-loop region. There is a poly (C) tract in the mtDNA control region which is interrupted by T at 16189 bp position in normal mtDNA sequences. Tumours 192 and 195 showed a consistent T deletion and varying sizes of poly (C) tract between 9 and 11 C nucleotides in heteroplasmic form. We found a C deletion at another poly (C) site at position nt303–309 in the D-loop region in cases 195 and 209. The mtDNA control region at nt514 encompasses a (CA)*n* repeat with five haplotypes. We found one and two CA insertions in two (192 and 105) of the six normal kidneys, respectively, but no allelic variation in the corresponding tumour cells.

***Somatic mtDNA mutations in ESRD/ACRD associated tumours*.** We identified nine somatic nucleotide changes occurring exclusively in tumour cells, eight of them in homoplasmic form (Table 7.). A G94A substitution was seen in tumour 192, a G16129A substitution in tumour 123B, a T16304C substitution in tumour 94B, and an A540G change in *MTTFH*, the mtTF1 (mitochondrial transcription factor 1) binding site H in tumour 123A, all in the mtDNA control region. A G4659A substitution occurred in the *MT-ND2* (mitochondrially encoded NADH dehydrogenase 2) coding region, leading to an amino acid exchange (Ala–Thr) in tumour 195, and a similar substitution, G5623A, was detected in the coding region for *MT-TA* (tRNA alanine) in tumour 105 (Figure 7).

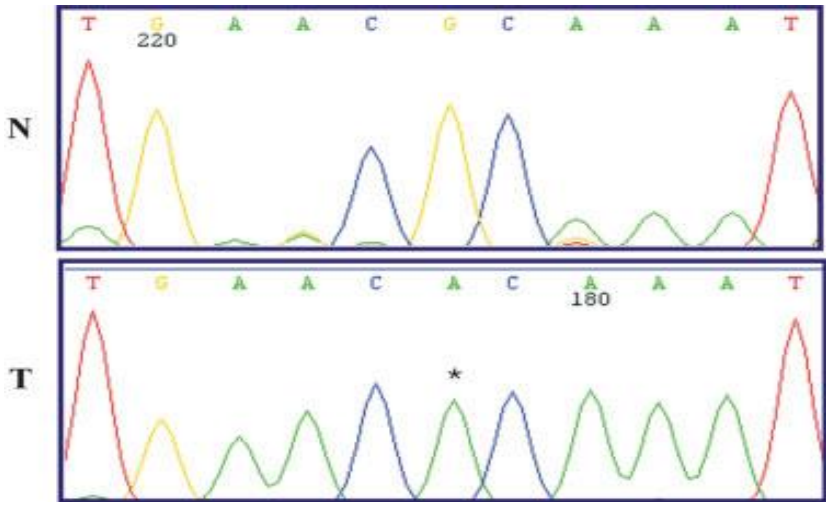

Figure 7. Results of mtDNA sequencing in case 105. Normal parenchymal cells (N) show a wild-type sequence, whereas tumour cells (T) have a G to A (*) transition at base position 5623 affecting the *MT-TA* (tRNA alanine) gene.

Tumour 123C showed a T insertion at position nt2978–2980 in the *MT-RNR2* (16S rRNA), whereas a C insertion occurred at bp 11 867–11 872 in the coding region for *MT-ND4* in tumour 94B. Finally, we found an A deletion in the polyA tract at position nt12418–12425, resulting in a frameshift mutation in *MT-ND5* in tumour 105. Repeated PCR amplification and sequencing of the mtDNA fragment from tumours and corresponding normal tissues confirmed the nucleotide changes.

Table 7. Somatic mtDNA mutations in RCTs from ESRD/ACRD kidneys

Tumor	***Location (nt)***	***nt-change***	***Amino acid change***	***Gene***
94 B	16304	T → C	NCR	D-loop
	C(11867 – 11872)	C insert	Frameshift aa372 of 460	MT-ND4
105 T	5623	G → A	NA	MT-TA
	12418	A8 → A7	Frameshift aa30 of 604	MT-ND5
123 A	540	A → G	NCR	MT-TFH
123 B	16129	G → A	NCR	D-loop
123 C	T (2978-2980)	T insert	NA	MT-RNR2
192 T	94	G → A	NCR	D-loop
195 T	4659	G → A	Ala - Thr	MT-ND2

Abbreviations: aa: amino acid; NCR: non-coding region; NA: not applicable; MT-ND4 / MT-ND5 / MT-ND2: mitochondrially encoded NADH dehydrogenase 4 / 5 / 2; MT-TA: mitochondrially encoded tRNA alanine; MTTFH: mitochondrially encoded transcription factor binding site H; MT-RNR2: mitochondrially encoded 16S RNA

3.5. Mutations of *VHL* and *MET* in ESRD/ACRD tumours

Mutation of the VHL gene. The coding region of the 3 exons of the VHL gene was sequenced directly from tumour DNA and the obtained sequences were aligned to the reference sequence (GenBank ID: NM_000551.2). In addition to the 11 tumours obtained from ESRD/ACRD patients, 128 conventional RCC from the general population were subjected to mutation analysis of the *VHL* gene. Altogether, 82 mutations within the three exons of the *VHL* gene occurring in 71 (55.5%) of the 128

tumours from the general population were detected. A point mutation occurred 45 times (54.9%), a deletion 30 times (36.6%) and insertion 7 times (8.5%) in the 71 conventional RCCs. Altogether 34 missense, 34 frameshift, 4 nonsense, 4 splicesite, 2 inframe and 1 silent mutation were detected. In seven tumours two mutations and in two cases 3 mutations (in two codons) were found. Loss of the 3p14.2-p25 region occurred in 97% of the 128 tumours (data not shown) whereas mutation of the *VHL* gene occurring only in 55.5% of the cases.

Sequence analysis of the three exons of the *VHL* gene in 6 conventional and 4 papillary RCCs as well as one oncocytoma from 7 ESRD/ACRD pateints revealed mutations exclusively in conventional RCCs. A point mutation of C819G occurred in tumour 94, whereas missense mutation with a cytosine>guanine change in exon 2 at codon 131 (606C/G) of the *VHL* gene in tumor 123B resulted in an asparagine>lysine change in the amino acid sequence. Tumour 137 displayed an nt732-736 (GAATT) deletion in exon 3 leading to a frameshift mutation (Figure 8). In tumor 192T, a deletion of 22 bp sequences in exon 3 (787delCCAAATGTGCAGAAGACCTGG) was detected, which resulted in a frameshift and finally, tumour 217 showed a T453A pointmutation in exon 1 of the *VHL* gene. Mutation of the *VHL* gene was found only in conventional RCCs of ESRD/ARCD patients and it seems to be higher in ESRD/ACRD associated conventional RCCs (83%) compatring to those occurring in the genertal population (55%).

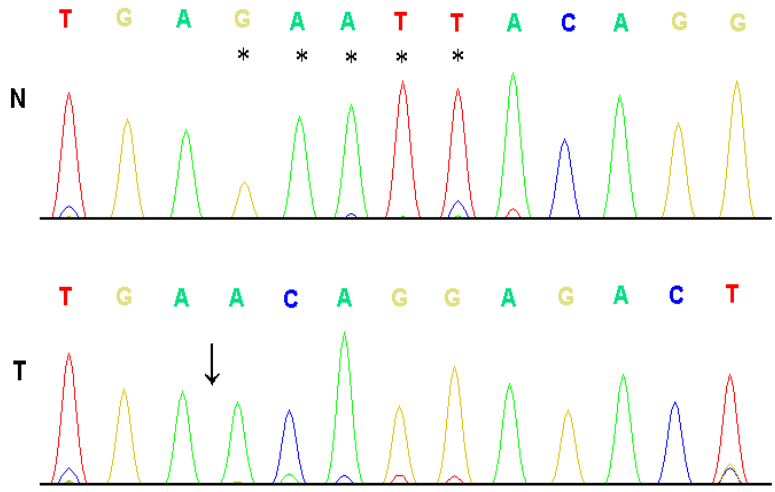

Figure 8. Deletion of nt732 – 736 (GAATT) in exon 3 of the *VHL* gene.

Mutation of the MET in ESRD/ACRD tumours. There were no any mutations in exon 16, 17, 18 and 19 of *MET* protooncogene of papillary renal cell tumors 94N, B, C, 123N, A, 203N, A, E.

3.6. Genomic alterations in ESRD/ACRD tumours

Twenty tumours from 11 patients with ESRD/ACRD were analysed for genomic DNA alterations. Examples are shown in Figure 9.

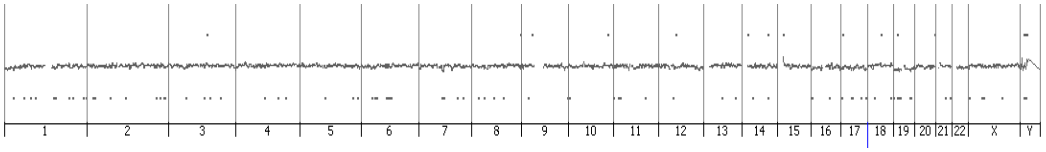

105

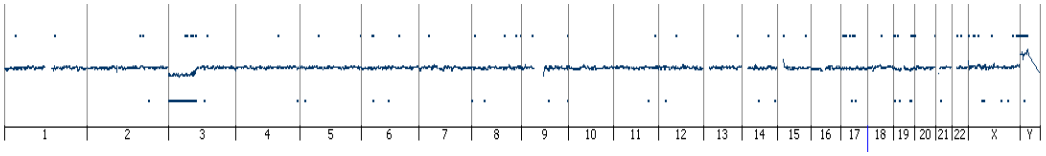

217

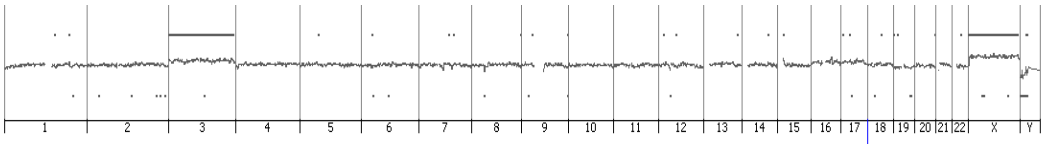

1926

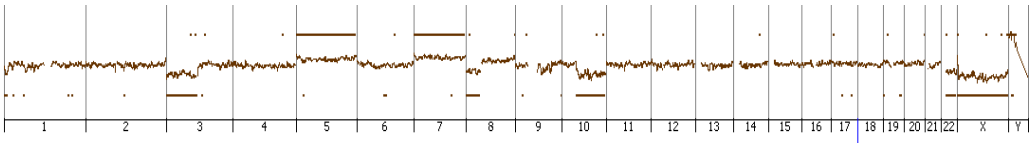

1400

Figure 9. Results of oligoarray CGH. No copy number changes were seen in the renal oncocytoma (105). Loss of chromosome 3p was the only alteration in a conventional RCC (217). The papillary RCC (1926) displayed only gain of chromosome 3 and the X chromosome. Another conventional RCC (1400) showed a complex DNA alteration including chromosome 3p loss.

Results of the genomic DNA alterations are shown in Table 8. Each of the 7 conventional RCCs displayed the characteristic copy number loss at chromosome 3p. However, only 2 (203A, E) of the 5 papillary RCTs showed the characteristic chromosomal gains whereas two of them (94B, 1926) displayed copy number gains only at chromosome 3, chromosomes 3 and 7 or chromosome 3 and 16. Of interest, the ACRD-associated eosinophilic tumour (123A) showed similar alterations to the papillary RCT 94B and 1926. Loss of chromosome 17p occurred frequently in chromophobe-like RCCs. No alterations were seen on the renal oncocytoma (105) and clear cell papillary RCT (123C).

Table 8. Genomic alterations in renal cell tumours from end stage kidneys

Tumour	Size (cm)	Diagnosis	Genomic changes
94A	0.8	cRCC	-3,+7,-Y
94B	0.2	pRCT	+7,+16q,-Y
94C	0.3	pRCT	none
105	4.0	RO	none
123 A	3.1	ACRD-ET	+3,+16
123 B	2.6	cRCC	-3,-14,-Y
123 C	2.2	ccpRCT	none
137	3.0	cRCC	-3p,+5q,-8p,-9p,-14q,-17,-20,-Y
173A	1.6	chRCC-like	-17p
173B	0.8	chRCC-like	-10,-2,-16q
173C	0.5	chRCC-like	-17p,-19
173D	1.0	chRCClike	none
173E	1.8	chRCC-like	-17p
192	3.5	cRCC	-3p,+7,+16q,-Y
195	3.0	cRCC	-3p,-14
203A	4.1	pRCT	+3,+5,+7,+16,+17,-Y
203E	0.3	pRCT	+3,+7,+8p,-14q,+16q
217	2.9	cRCC	-3p
1400	3.8	cRCC	-3p,+5,+7,-8p,-10q,-X
1926	3.6	pRCT	+3,+X

3.7. Expression signature of end-stage kidneys

3.7.1. Correspondence analysis

To identify the genes associated with the remodelling processes and increased tumourigenesis we have compared the expression profile of ESRD/ACRD kidneys to those of normal kidneys and RCTs obtained from the general population by using the oligonucleotide microarray technology. Correspondence analysis of normal foetal, adult and ESKD/ACRD kidneys and distinct types of kidney tumours revealed 5 sample clusters (Figure 10).

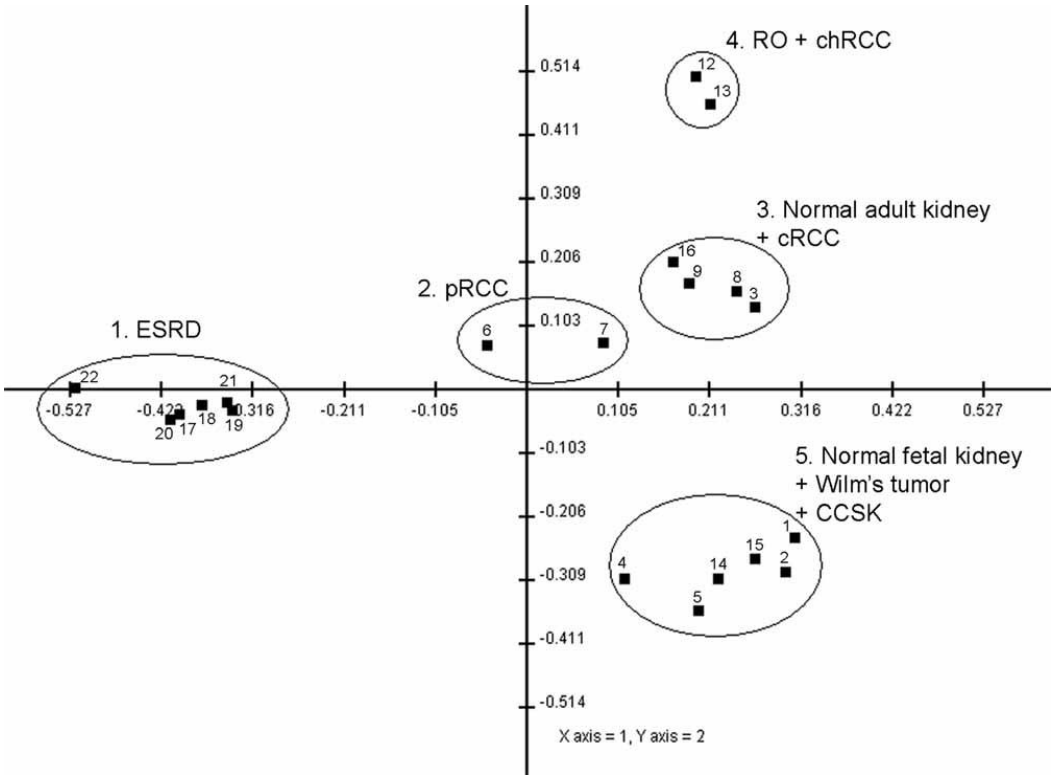

Figure 10. Correspondence analysis of the microarray experiments. The five clusters are highlighted with a solid line circles. Samples 17-22 in cluster 1 corresponding to ESRD/ACRD are localized far from the centroid and other clusters indicating an unique expression signature. The number of samples corresponds to those shown in Table 4.

All samples and genes without filtering is shown in Figure 10, which was drawn after zooming in on its center to clearly reveal the 5 sample clusters, cutting highly differential genes at the top, bottom, and right margin of the plot. The conformation of the plotted objects after filtering out approximately 80% of the genes for low transcription did not change much, corroborating the stability of the identified clusters. This analysis showed that ESRD/ACRD (cluster 1, samples 17-22 in Figure 10) has unique transcription profile, well separated from the other clusters containing normal and tumourous conditions of the kidney.

We have selected 69 genes based on the signal log ratio and detection calls, which are specifically up-regulated in ESRD/ACRD against normal adult kidneys and down-regulated in RCTs of the general population. Quantitative RT-PCR analysis using a panel of cDNA from normal and ESRD/ACRD kidneys and distinct type of RCTs confirmed the 2 to 208-fold expression of 47 genes (Table 9). Twenty-one of the 47 genes were expressed exclusively in ESRD/ACRD, whereas 26 other genes were also expressed in one or more types of RCTs as well. Of interest, 9 of the 26 genes were expressed exclusively in ESRD/ACRD and in papillary RCCs suggesting an association between the two diseases. The highest expression in ESRD/ACRD was seen for the *LINC00973* RNA (Long Intergenic Non-Protein Coding RNA 973; formerly Hs.307772), followed by the *CSF2, SCEL* and *GPR87* genes. None of the childhood and adult renal tumors obtained from the general population displayed expression of the *LINC00973*, *CSF2* and *GPR87* sequences, whereas the *SCEL* was overexpressed in papillary RCTs as well.

Table 9. Relative expression of genes in ESRD/ACKD kidneys and RCTs of the general population as validated by quantitative RT-PCR

Gene symbol	ESKD/ACKD	pRCT	cRCC	chRCC	RO
LINC00973	208+	-	-	-	-
CSF2	167	-	-	-	-
SCEL	137	191	-	-	-
GPR87	128	-	-	-	-
KRTAP2-2	17	-	-	-	-
TRPM8	17	39	4	3	3
PMAIP1	16	-	-	4	-
CXCL5	16	6	5	-	-
NPFFR2	16	-	-	-	-

GJB3	15	6	-	-	-
AHNAK2	14	35	18	-	-
FOXE1	13	-	-	-	-
AREG	13	-	-	-	-
CXCL8	11	-	-	-	-
NCAPG	11	3	3	2	2
APOBEC3B	11	3	4	6	-
NDC80	10	-	4	-	-
ALDH1A3	10	-	-	-	-
LAMA3	9	13	-	-	-
TACC3	9	-	4	2	-
EREG	9	12	6	-	-
CXCL6	9	13	-	-	-
KRT81	8	5	-	-	-
KRT19	7	3	-	-	-
DCBLD2	7	3	-	-	-
IL6	7	-	3	-	-
CCL20	6	-	6	-	-
SERPINB7	6	-	-	-	-
LINC00521	6	2	4	-	-
CXCL1	6	-	-	-	-
WNT7A	6	-	-	-	-
CST6	5	-	-	-	-
TMEM154	5	-	-	-	-
NOG	5	3	-	2	-
CENPK	5	2	3	-	-
LAMB3	4	-	-	-	-
PDLIM4	4	-	-	-	-
SHISA9	4	-	4	-	-
KRT23	3	-	-	-	-
LAMC2	3	5	-	-	-
CLEC4E	3	-	-	-	-
RAB3B	3	-	-	3	13
ULBP2	3	-	4	-	-
ATAD2	3	-	-	-	-
CXCL3	2	-	-	-	-
ASPM	2	-	-	-	-
KRT7	2	2	-	-	-

[+]Fold expression of genes correlated to the expression in normal kidneys.

3.7.2. Unsupervised hierarchical clustering

After normalizing the data to the expression level in normal kidneys, unsupervised analysis revealed distinct global gene expression patterns of ESRD/ACRD/papillary RCC, chromophobe RCC/renal oncocytoma, conventional RCC, and foetal kidneys together with the childhood tumours as grossly separated clusters (Figure 11).

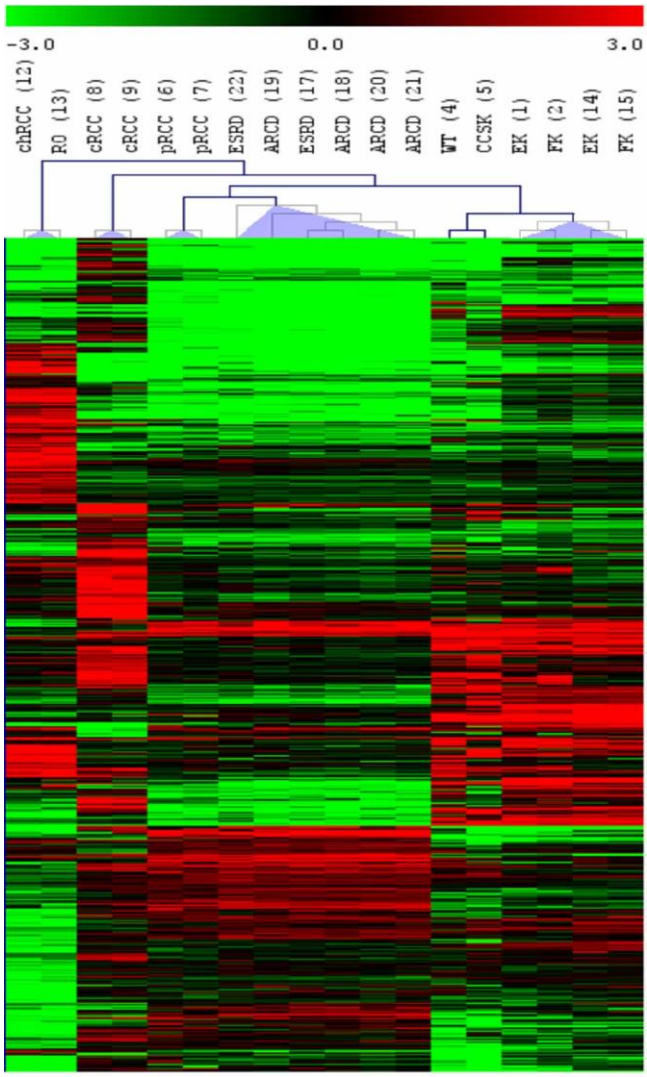

Figure 11. Hierarchical clustering tree of the microarray-based expression profiles. Cluster obtained for the transcripts of ESRD/ACRD is overlapping with that of papillary RCT. The samples joined by very short branches have gene expression patterns that are very similar to each other and by increasingly longer branches their similarity decreases.

The SAM analysis with the available number of permutations and fold-change 2.0 was performed to estimate a statistical significance of the probe sets manually selected as transcripts associated with ESRD/ACRD and ESRD/ACRD and papillary RCC. As result, 54 and 42 transcripts were up-regulated in ESRD/ACRD and ESRD/ACRD and papillary RCC, respectively, as compared to other samples (Figure 12).

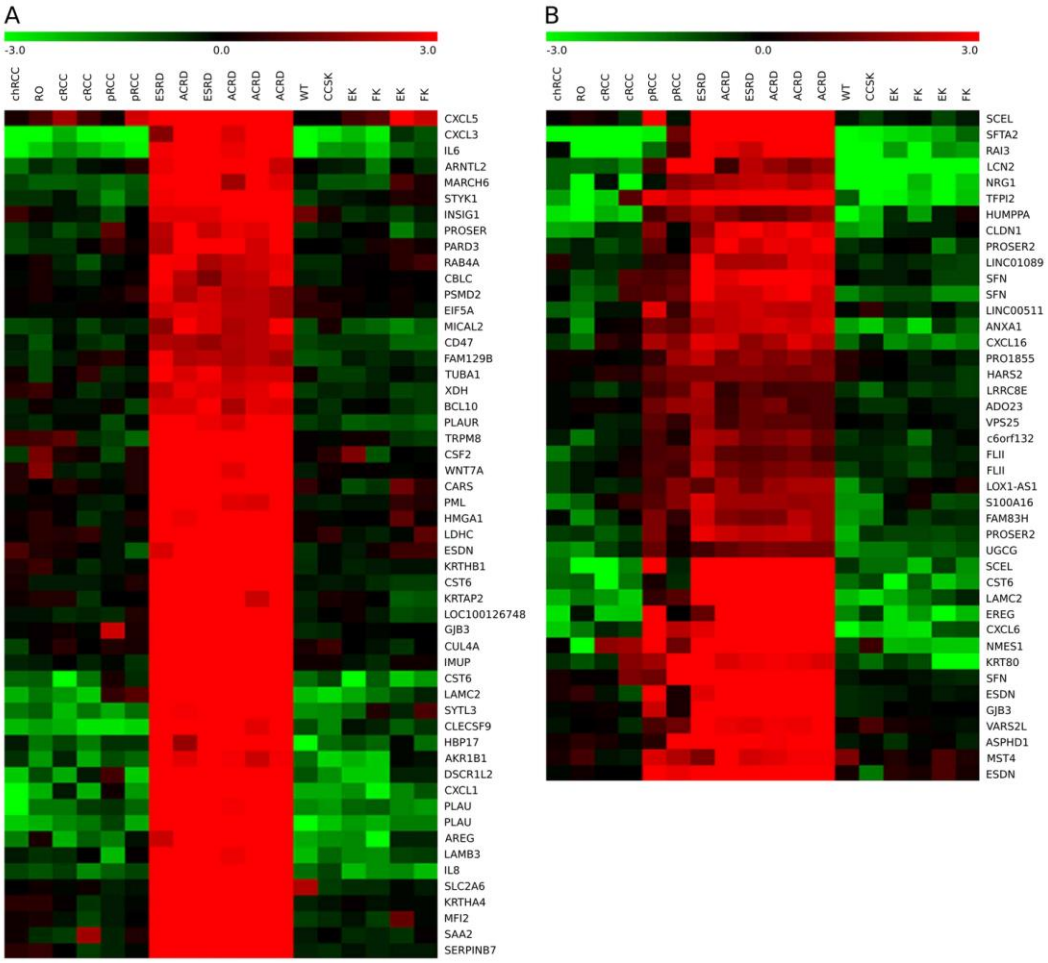

Figure 12. A, mRNA sequences identified by SAM. 54 mRNA sequences were identified which are up regulated in ESRD/ACRD against other tissue probes. Note the specific expression of genes in ESRD/ACRD kidneys (in red). The ID number of probes corresponds to those are listed in the legend of Figure 1. B, mRNA sequences identified by SAM. Evaluating the expression of genes specifically upregulated in ESRD/ACRD and papillary RCCs against other tissue probes revealed 42 genes (in red).

3.8. Analysis of most prominently expressed genes

Table 10. Samples used for RT-PCR to confirm the most prominently expressed genes.

	Sample
1	Normal kidney, 13 weeks old fetus
2	Normal kidney, 18 weeks old fetus
3	Normal kidney, 19 weeks old fetus
4	Normal adult kidney, 279N
5	Normal adult kidney, 332N
6	Normal adult kidney, 343N
7	Normal adult kidney, 344N
8	Normal adult kidney, 462N
9	ESRD kidney, HD94N
10	ACKD kidney, HD105N
11	ACKD kidney, HD123N
12	ESRD kidney, HD137N
13	ACKD kidney, HD195N
14	ACKD kidney, HD 209N
15	ESRD kidney, HD217N
16	ESRD kidney, HD232N
17	Rhabdoid tumour of the kidney, HD4
18	Wilms' tumour, HD9
19	Wilms’ tumour, HD496
20	Papillary renal cell tumour, HD92T
21	Papillary renal cell tumour, HA425T pT3,G3
22	Papillary renal cell tumour, HA426T
23	Papillary renal cell tumour, HA455T
24	Papillary renal cell tumour, HA456T
25	Papillary renal cell tumour, HD1510T
26	Renal “Loopoma”, HD1847T
27	Clear cell sarcoma of the kidney, HA302
28	Conventional RCC, HA279T
29	Conventional RCC, HA332
31	Conventional RCC, HA344T
31	Conventional RCC, HA395T
32	Conventional RCC, HA400T
33	Chromophobe RCC, HD88T
34	Chromophobe RCC, HA244T
35	Chromophobe RCC, HA315T

36	Chromophobe RCC, HA417
37	Renal oncocytoma, HD30
38	Renal oncocytoma HD171T
39	Renal oncocytoma, HA381T
40	Renal oncocytoma, HD661T
41	Renal oncocytoma HD1175T

Table 11. Samples used to establish the gene expression in ESRD/ACRD associated tumours.

	Sample
1	Normal kidney, 13+19 weeks old fetus
2	Normal adult kidney, HD112N
3	Normal adult kidney, HD182N
4	Normal adult kidney, HD182N
5	Normal adult kidney, HD194N
6	Normal adult kidney, HS271N
7	Normal adult kidney, HA322N
8	Normal adult kidney, HA343N
9	ESRD kidney, HD94N
10	ESRD kidney cyst wall, HD94N
11	ACKD kidney, HD105N
12	ACKD kidney, HD123N
13	ESRD kidney, HD137N
14	ACRD kidney, HD192N
15	ACKD kidney, HD195N
16	ESRD kidney, HD 203N
17	ESRD kidney, HD217N
18	ESRD kidney, HD1871N
19	ESRD kidney, HD1923
20	ACKD kidney, HD1926
21	ACRD-associated T, HD123A
22	ccpRCC, HD123C
23	Renal oncocytoma, HD105A
24	Papillary RCT, HD203A
25	Papillary RCT, HD1926
26	Conventional RCC, HD123B
27	Conventional RCC, HD137T
28	Conventional RCC, HD217T
29	Conventional RCC, 1871T
30	Conventional RCC, 1923T

3.8.1. *LINC00973* (Hs.307772)

LINC00973 is a Long Intergenic Non-Protein Coding RNA 973 located on the positive strand of chromosome 3 at base pairs 98699902-98701940. *LINC00973* is an RNA gene containing sequences, which probably targeted by hsa-miR-449b, hsa-miR-3153 and hsa-miR-4679. *The LINC00973* belongs to the non coding RNA seqeunces which are conserved in mouse and also in fish. The function of the *LINC00973* sequences are not yet known, no data on its involvement in any biological functions has been published. We found the expression of *LINC00973* exclusively in ESRD/ACRD kidney. Q-RT-PCR failed to detect *LINC00973* molecules in embryonal and adult kidney, Wilms' tumour and distinct types of renal cell tumours of the general population (Figure 13). However, when comparing normal and end stage kidneys and ESRD/ACRD associated tumours, expression of the *LINC00973* was detected in five of the ten ESRD/ACRD associated tumours. (Figure 14).

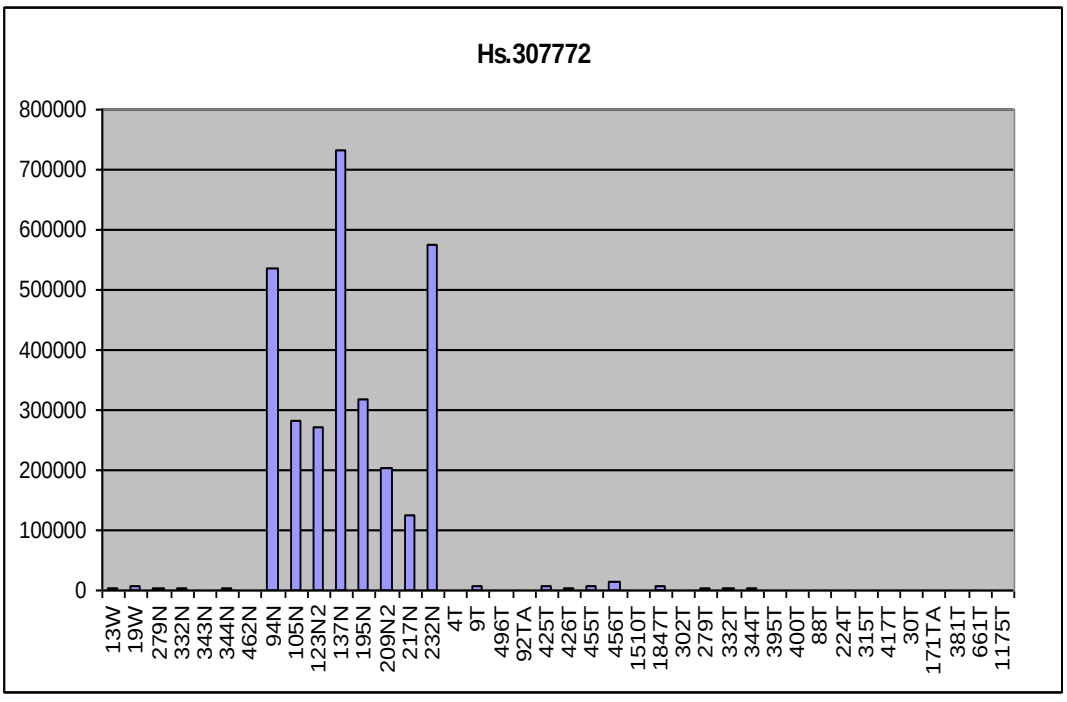

Figure 13. High expression of the *LINC00973* (Hs.307772) in ESRD/ACRD kidneys (94N-232N).

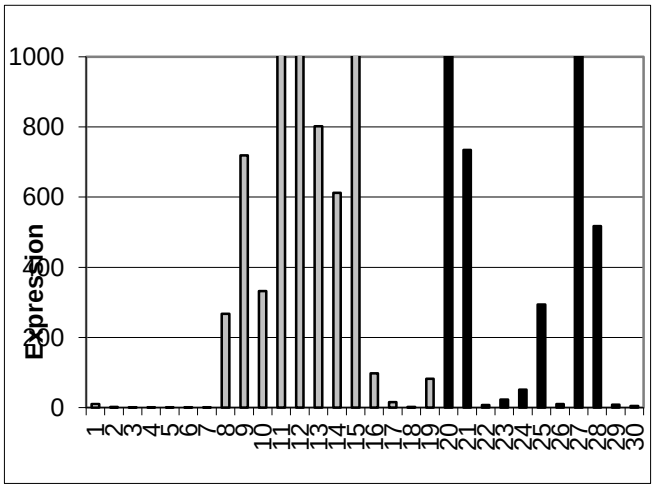

Figure 14. Expression of *LINC00973* in normal kidneys (1-7), ESRD/ACRD (8-19) and ESRD/ACRD associated tumours (20-30).

3.8.2. Colony Stimulating Factor 2 *(CSF2)*

The granulocyte-macrophage colony stimulating factor 2 (*GM-CSF* or *CSF2*) has a cytokine function controlling the differentiation and function of granulocytes and macrophages. It was shown earlier that *CSF2* is expressed in renal tubular cells after acut ischemic injury and activated unique macrophage "reparative" phenotype that supported tubular proliferation.We detected *GM-CSF* mRNA by RT-PCR in cultured human renal cells, but not in kidney tissue. Q-RT-PCR analysis of the panel of normal kidneys and tumours revealed *CSF2* expression exclusively in the ESRD/ACRD kidneys. No expression was seen in tumour samples from the general population. (Figure 15)

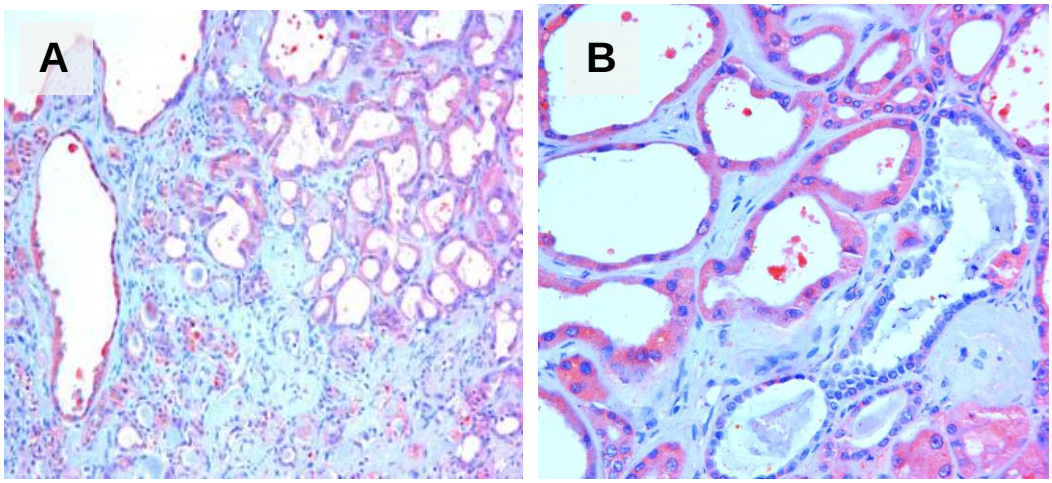

Figure 15. Diffuse expression of the CSF2 protein in atrophic, rearranged and cystic dilated tubuli.

3.8.3. Sciellin (*SCEL*)

Expression of SCEL in ESRD/ACRD kidneys and tumours. The protein encoded by *SCEL* is a precursor protein to the cornified envelope of terminally differentiated keratinocytes. This protein localizes to the periphery of cells and may function in the assembly or regulation of proteins in the cornified envelope. It was shown the *SCEL* is expressed only in cornified epithelial cells of the skin, vagina, esophagus and tumours arising from such cells. Therefore, it is not expected to be expressed in parenchymal organs. Surprisingly, the sciellin was the third most prominently expressed gene identified by Affymetrix array and Q-RT-PCR analysis in ESRD/ACRD kidney. We have also found a consequent *SCEL* expression in papillary RCT of the general population but not in conventional and chromophobe RCCs or renal oncocytomas (Figure 16). The cornified envelope of keratinocytes is an insoluble protein structure formed under the plasma and a major component of the chemical and physical barrier of the skin. A number of these proteins are crosslinked into the envelope by the enzyme transglutaminase 1. The central domain of the *SCEL* encompasses 16 repeats of 20 amino acids rich in Gln and Lys residues which may be potential transaminase substrates.

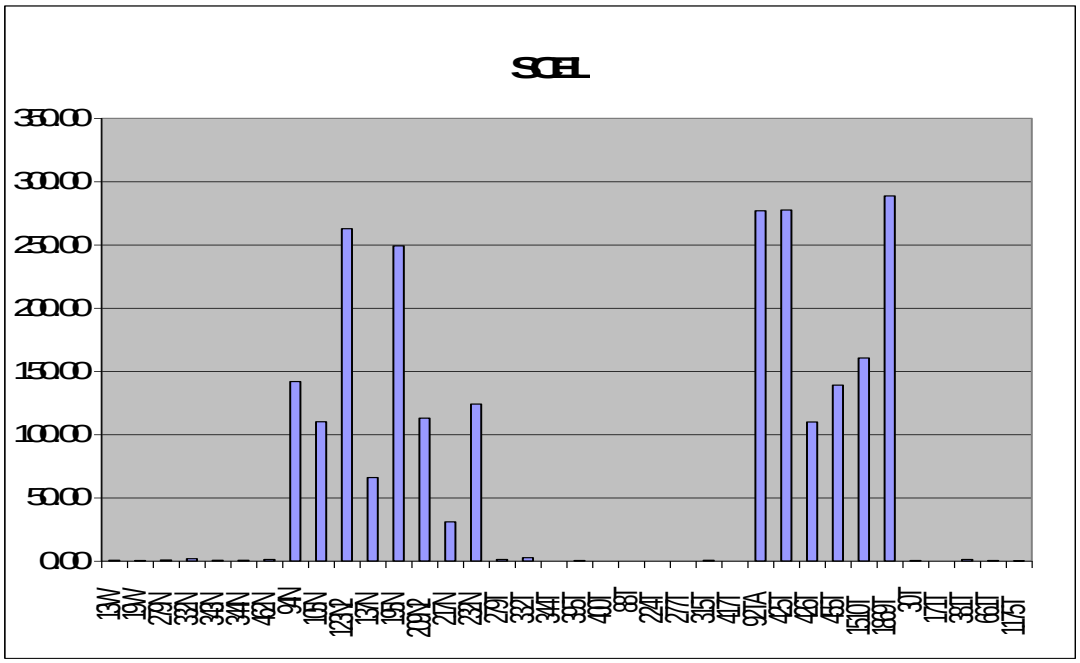

Figure 16. Results of Q-RT-PCR analysis. Note the expression of *SCEL* in ESRD/ACRD kidneys (94N-232N) and papillary RCTs (92TA-1869T).

In addition, we have analysed the *SCEL* expression in 11 tumours developed in ESRD/ACRD kidneys (Figure 17). Again, no expression was seen in normal foetal and adult kidneys whereas 10 of the 12 ESRD/ACKD kidneys expressed the *SCEL* gene. A high copies of *SCEL* molecules were detected also in 5 of the 11 ESRD/ACRD associated tumours including ACRD associated papillary clear cell tumour and also a tumour with large vacuolized eosinophilic cells. These data suggest the possible role of *SCEL* in the proliferative processes playing a role in development of ESRD/ACRD and associated tumours. The C-terminal region of the *SCEL* contains one highly conserved LIM domain that is found in a number of genes involved in regulation of cell proliferation and differentiation. The *LIM1 (LHX1)* homeobox gene is temporally and spatially expressed in comma and S-shaped bodies of human kidneys between 10 and 30 weeks of gestation, but the expression is diminished in adult kidneys as well as in conventional and papillary RCCs arising in the general population.

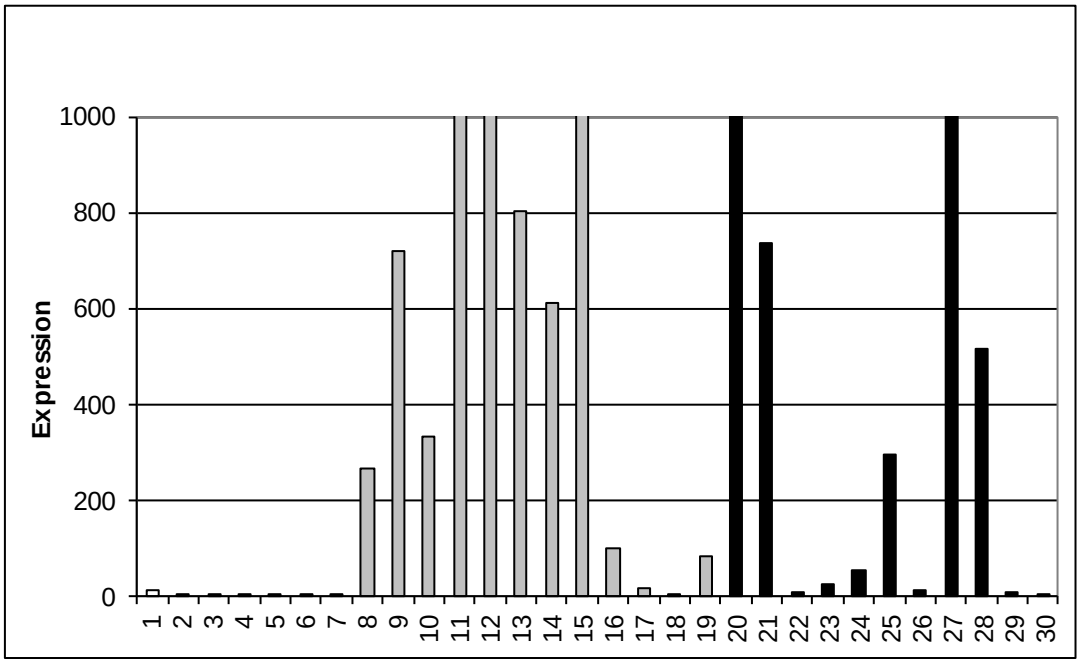

Figure 17. Q-RT-PCR analysis of *SCEL* expression. Note the extremly low expression in normal kidneys (1-7) and the high expression in ESRD/ACRD kidneys (8-19) and associated tumours (20-30).

Two transcript variants of the *SCEL* utilizing an alternative polyA signal has been described in the literature but the biological function of the two isoforms has not been cleared. We have analysed the expression of the two splice variants of the *SCEL* by RT-PCR and the fragments were visualised on agarose gel. Correspondingly to the result of Q-RT-PCR, no visible expression was seen in normal foetal and adult kidneys, Wilms' tumors, conventional and chromophobe RCCs and renal oncocytomas after 30 cycles of amplification. Although the expression of both splice variants was detected, a strong predominance of the variant 2 with insertion of exon 12 was seen in each of the eight ESRD/ACRD kidneys and of five papillary RCTs obtained from the general population (Figure 18).

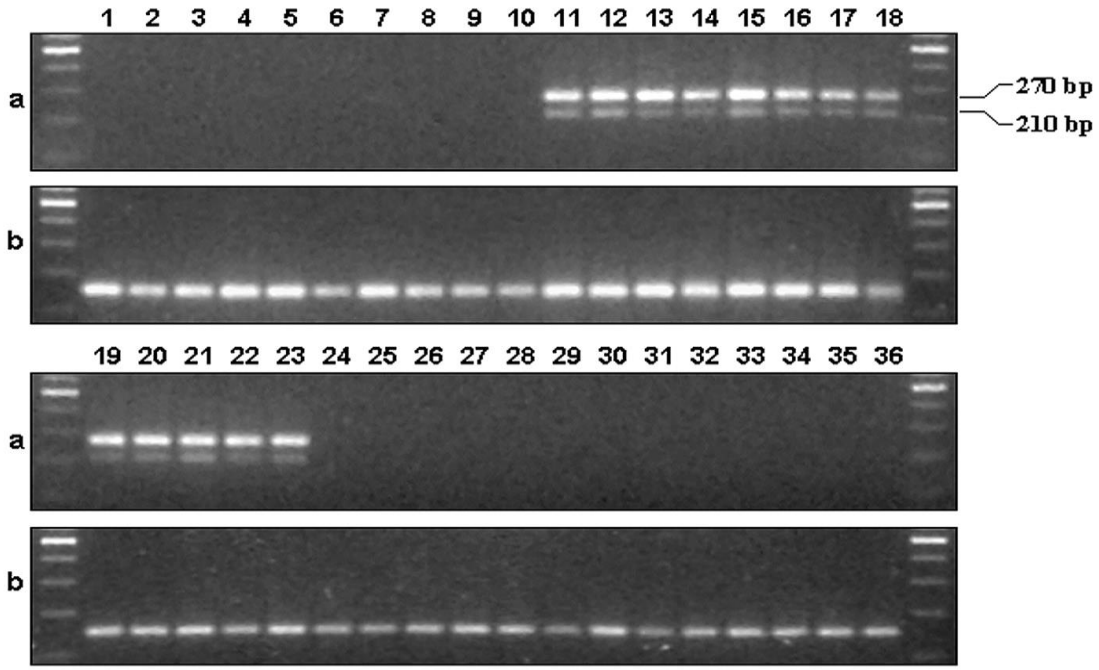

Figure 18. RT-PCR analysis of the expression of transcript variant 1 (210 bp) and variant 2 (270 bp) of the gene *SCEL*. Samples of the series: foetal kidneys (1-2), Wilms' tumours (3-5), normal adult kidneys (6-10), ESRD/ACKD kidneys (11-18), papillary RCTs (19-23), conventional RCCs (24-28), chromophobe RCCs (29-32) and renal oncocytomas (33-36). Notice the strong expression of splice variant 2 of the *SCEL* in end-stage kidneys and papillary RCTs (a). The β-actin was ubiquitously expressed in all tissues (b).

Expression of sciellin protein in ESRD/ARCD and renal cell tumours. Because of its high expression in ESRD/ACRD kidneys and papillary RCTs and the strong association of papillary RCTs and ESRD/ACRD, we have analyzed the cellular localization of sciellin by immunohistochemistry. In adult kidneys a positive staining was seen exclusively in distal convoluted tubuli (Figure 19A). In ESRD associated sclerotic renal parenchyma single or clustered epitheloid cells resembling Selye's endocrine kidneys displayed a high expression of sciellin protein (Figure 19B). At the beginning of cystic changes several dilated distal tubuli contained small papillary cell proliferations within their lumen (Figure 19C). We found cytoplasmic and membrane bound positivity in papillary RCCs arising in ESRD/ACRD (Figure 19 D). None of the 45 conventional and 8 chromophobe RCCs, 8 renal oncocytomas and 4 Wilms' tumors arising in the general population was positive for SC4 antibody. We

have analysed 25 small papillary precursor lesions detected in ESRD/ACRD kidneys. Twenty three lesions were consisted of small cells with scanty cytoplasm resembling embryonal rests, all of them were positive for SC4 antibody Precursor lesions for ACRD-associated eosinophilic-vacuolated tumor and also the tumors itself displayed a cytoplasmic staining for sciellin. The ACRD-associated papillary clear cell tumor was negative for sciellin.

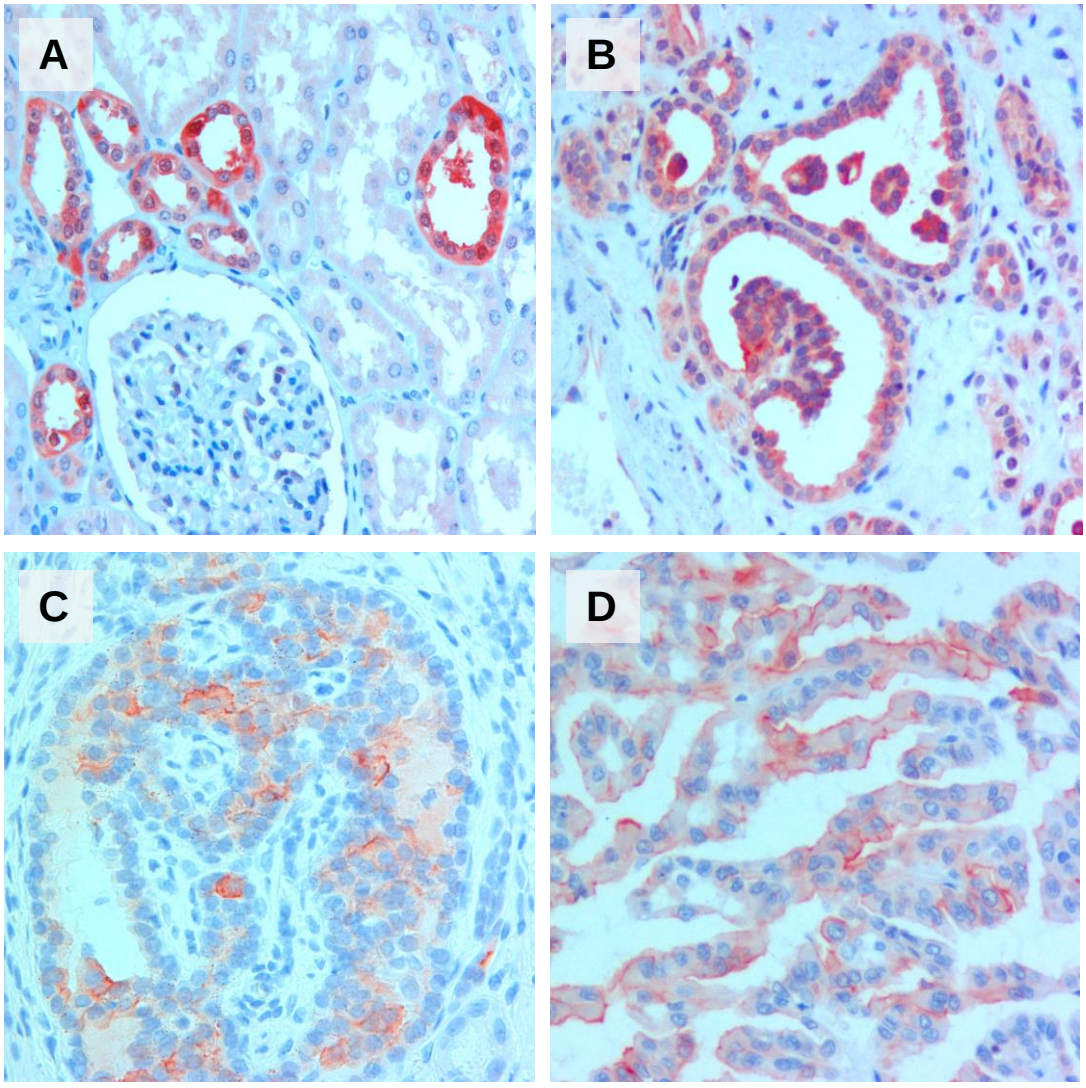

Figure 19. Immunohistochemistry of sciellin. Distal tubular cells of normal kidney are strongly positive for SC4 antibody (A). In scarring end stage kidney small tubules and also a dilated tubulus containing a papillary growthe of cells were postive (B). A larger papillary precursor lesio (C) as well a papillary RCT (D) displayed positive staining.

Expression of SCEL and Vitamin D upregulated protein 1 (VDUP1) in ESRD/ACRD kidney. We have analysed the same panel of normal and ESRD kidney and distinct types of tumour samples for SCEL and *VDUP1/TXNP* by quantitative RT-PCR (Figure 20, Figure 21).

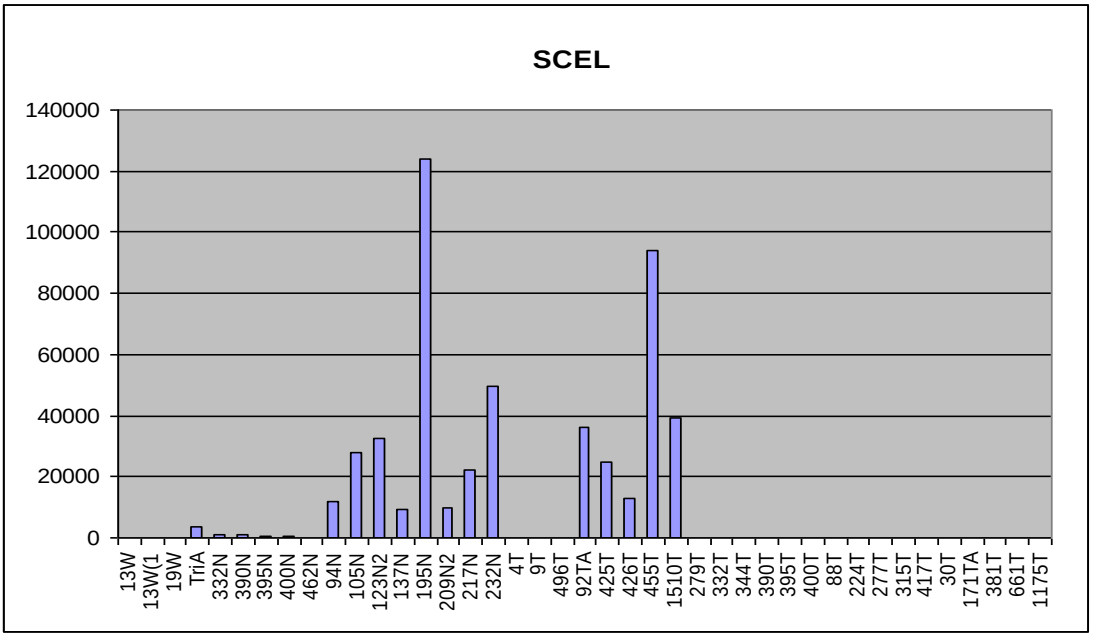

Figure 20. Expression of *SCEL* in ESRD/ACRD kidney (94-232) and papillary RCT (92A-1510).

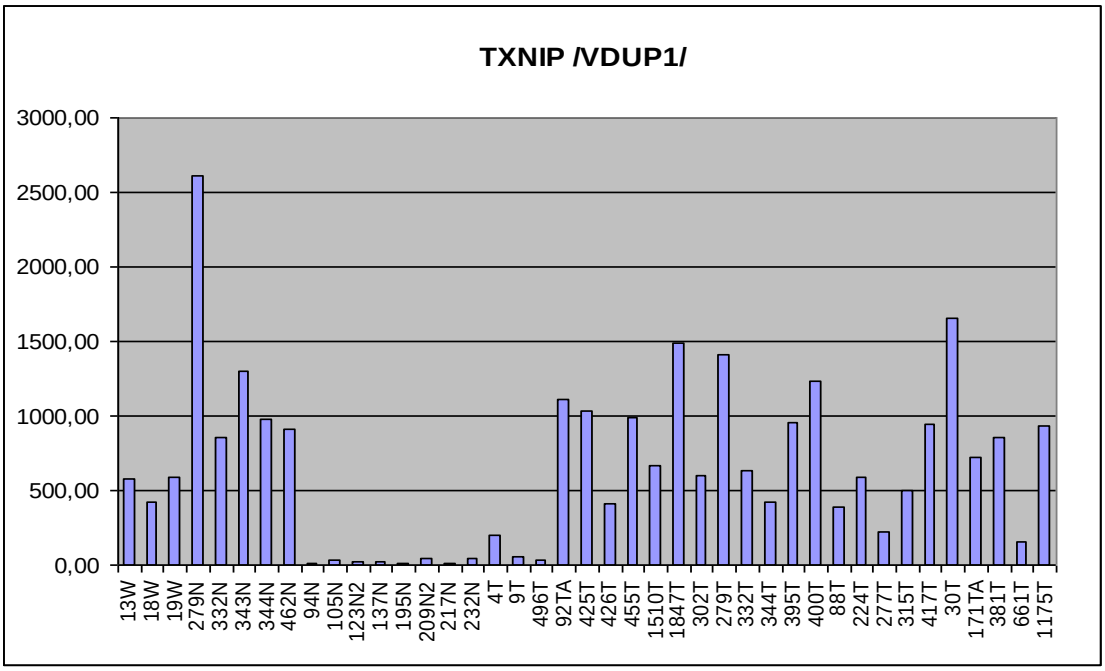

Figure 21. Expression of *TNXP/VDUP1*. Note the low expression of the *TXNP/VDUP1* in ESRD/ACRD kidneys (94N-232N).

The interaction of SCEL with *VDUP1/TXNIP* and the low serum level of 1α, $25(OH)_2D_3$ in patients with end stage renal disease promted us to analyse the *VDUP1/TXNIP* expression in a panel of samples including ESRD/ARCD kidneys. We found a *VDUP1/TXNP* expression in all normal kidneys and also distinct types of renal cell tumours but no or very low expression in ESRD/ACRD kidneys (Figure 21, 94N-232N) and Wilms tumours (Figure 21, 4T-496T).

3.8.4. G Protein-Coupled Receptor 87 (*GPR87*)

GPR87 was the third most prominently expressed gene in our panel. The G protein-coupled receptor is mapped to a cluster of G protein-couple receptor genes on chromosome 3. The encoded protein has been shown to be overexpressed in lung squamous cell carcinoma and urothelial carcinoma. We have detected the expression of *GPR87* in ESRD/ACRD kidneys with global gene expression analysis and confirmed by Q-RT-PCR (Figure 22). *GPR87* contributes to viability of human tumor cells and it is necessary for p53-dependent cell survival in response to genotoxic stress.

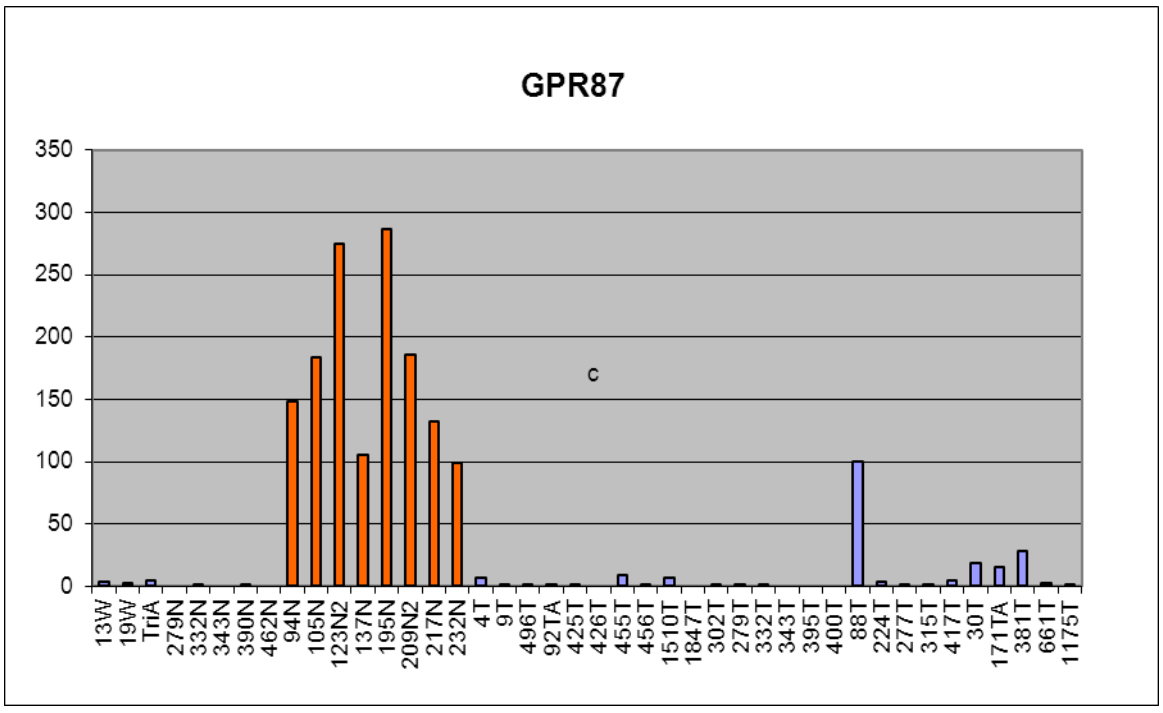

Figure 22. Note the high expression of *GPR87* in end stage kidneys (94N-232N) and also in a collecting duct carcinoma (88T). Three oncocytomas (30-381) also display a weak expression of the *GPR87*.

Immunhistochemical analysis revealed a strong reaction with GPR87 antibody in the vas afferens of cortical glomeruli in adult kidneys and a week reaction in cells of outer medullary collecting duct of fetal and adult kidneys (Figure 23 A and C). A strong positivity was seen in small proliferating arterioles correponding to the outer medullary region in ESRD/ACKD kidneys (Figure 23 B) and also in chromophobe RCC-like precursor lesions and tumours (Figure 23 D).

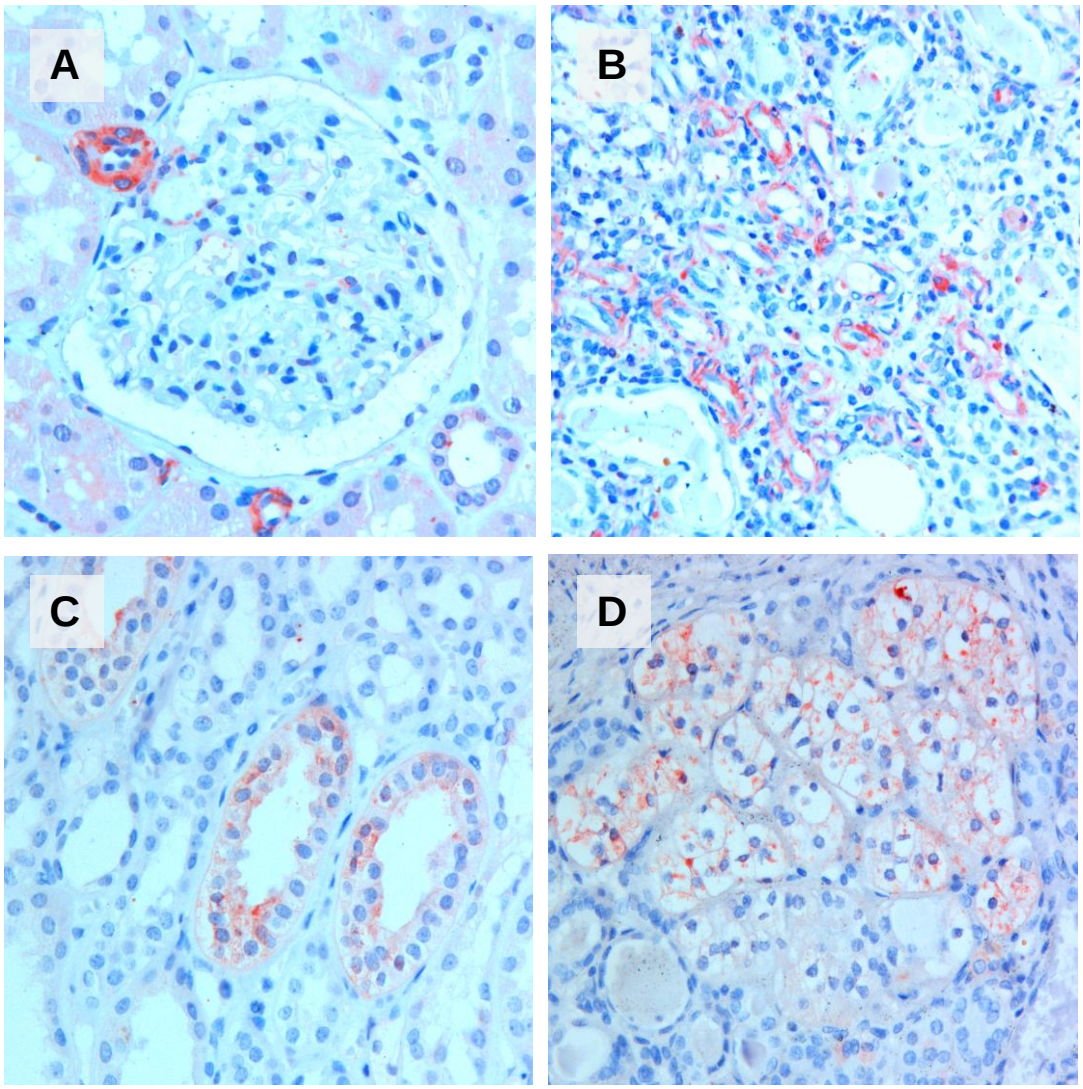

Figure 23. Immunohistochemistry of *GPR87*. There is a strong immunopositivity with GPR87 antibody in cells of the vas afferens connected to the glomerulus (A). Proliferating small blood vessels embedded in scarring stroma in ESRD reveal positive staining with *GPR87* (B). Cells of the collecting duct (C) as well as chromophobe-like precursor lesion show weak cytoplasmic and attenuated membrane positivity with *GPR87* antibody.

3.9. Functional classification of selected genes

The differentially expressed genes identified using quantitative fold-change criteria and qualitative metrics and improved by Q-RT-PCR in a panel of samples and those subsequently selected by the significance analysis of microarrays were subjected to the functional analysis. To define functionally related genes among those specifically expressed in ESRD/ACRD kidneys used web-based DAVID Gene Functional Classification Tool (67).

We identified two clusters of functionally related genes among the 47 genes confirmed by Q-RT-PCR (Table 12). Five genes of chemokines (chemotactic cytokines), *CXCL1, CXCL3, CXCL5, CXCL6* from the C-X-C subfamily and CCL20, a member of the C-C subfamily were clustered together with a high enrichment scores (essentially, a variant of Fisher exact probability) when classification stringency was set as "highest". In addition, *CXCL8 (IL8)* was also assigned to the cluster of "high" stringency level. These genes were overexpressed in ESRD/ACRD kidneys alone (*CXCL1, CXCL3, IL8*) or simultaneously in papillary and/or in conventional RCCs. Two of the 47 genes overexpressed in end-stage kidneys based on qRT-PCR analysis, *CSF2* and *IL6* can be referred here as well, which encode also proteins belonging to the large group of cytokines. All these genes are known to be inflammatory cytokines

Another cluster was made up by keratins, *KRT7, KRT19, KRT81 (KRTHB1),* and *KRT23* at "highest" clustering stringency settings, and *KRTAP2-2* at a stringency set to "high". *KRTAP2-2, KRT81 and KRT23* were overexpressed exclusively in ESRD/ACRD kidneys, while *KRT19* and *KRT7* expressed in papillary RCTs as well. Based on the role of encoded proteins in epidermal development and maintainance, the *SCEL* as well as C15orf48 (*NMES1*, normal mucosa of oesophagus specific 1) might also be ordered to this functional group. The gene *AREG* encodes an autocrin growth factor promoting the growth of normal epithelial cells. Of interest, the *KRT8* and *KRT18*, which are normally expressed in single layered epithelial cells such as renal tubules, are not overexpressed in ESRD/ACRD kidneys.

Table 12. Functional classification of differentially expressed genes*

Gene symbol	Affymetrix ID	Kappa (similarity score)
Functional group 1, enrichment score 4.77		
CCL20	205676_at	0.65
CXCL6	206336_at	0.57
CXCL5	207852_at	0.64
	214974_x_at	
	215101_s_at	
CXCL1	204470_at	0.57
CXCL8	202859_x_at	0.40
	211506_s_at	
CXCL3	207850_at	0.74
Functional group 2, enrichment score 3.57		
KRT19	201650_at	0.67
	228491_at	
KRT81	213711_at	0.59
KRT23	218963_s_at	0.70
KRT7	209016_s_at	0.70
	214031_s_at	
KRTAP2-2	234772_s_at	0.42

***** DAVID scored one to three Hs. sequences to the two functional groups of cytokines and keratins with high similarity score.

3.9.1. Group 1: Inflammation related genes

The DAVID analysis of ESRD-ACRD associated genes uncovered a functional group of cytokines, which are known to be involved in inflammatory processes. Quantitative RT-PCR analysis confirmed the high expression of *CXCL1, CXCL3, CXCL5, CXCL6* and *CXCL8* as well as of *CCL20* in ESRD/ACRD kidneys and also in associated renal cell tumours. No or only minimal expression was detected in normal, non-ESRD/ACRD kidneys. These data suggest that inflammatory cytokines may play a seminal role in the remodelling processes in ends stage kidneys and also in development of ACRD. Moreover, we found a high expression of the aforesaid cytokines in distinct types of renal cell tumours which developed in ESRD/ACRD kidneys.

Expression and cellular localisation of CXCL8 and CXCR2. As *CXCR2 (IL-8R2*) is a receptor for *CXCL3, CXCL5, CXCL6* and *CXCL8*, we have analysed the receptor protein together with the *CXCL8* cytokine in the same slides by immunohistochemistry in ESRD/ACRD kidneys and associated tumours. Adult and fetal kidneys were negative for *CXCL8*. End stage kidneys revealed only scattered positivity for both *CXCL8* and its receptor *CXCR2* in areas with thyroid-like structures. The vast majority of small "atrophic" tubules in sclerotic areas and small tubular and tubular-papillary lesions were positive for both antibodies. ESRD/ACRD associated precursor lesions as well as small tumors resembling chromophobe RCC showed positive staining for both antibodies. Several tubular-papillary lesions of small cells, which are frequently seen in association with clinically recognized papillary RCT, were also positive for *CXCL8* and *CXCR2*. Smaller or larger cyst in ACRD kidneys lined with single or multilayered epithelial cells were strongly positive. In summary, similar structures were stained with both antibodies being the staining intensity for *CXCR2* generally weaker than for its ligand *CXCL8*. Examples are shown in Figure 24.

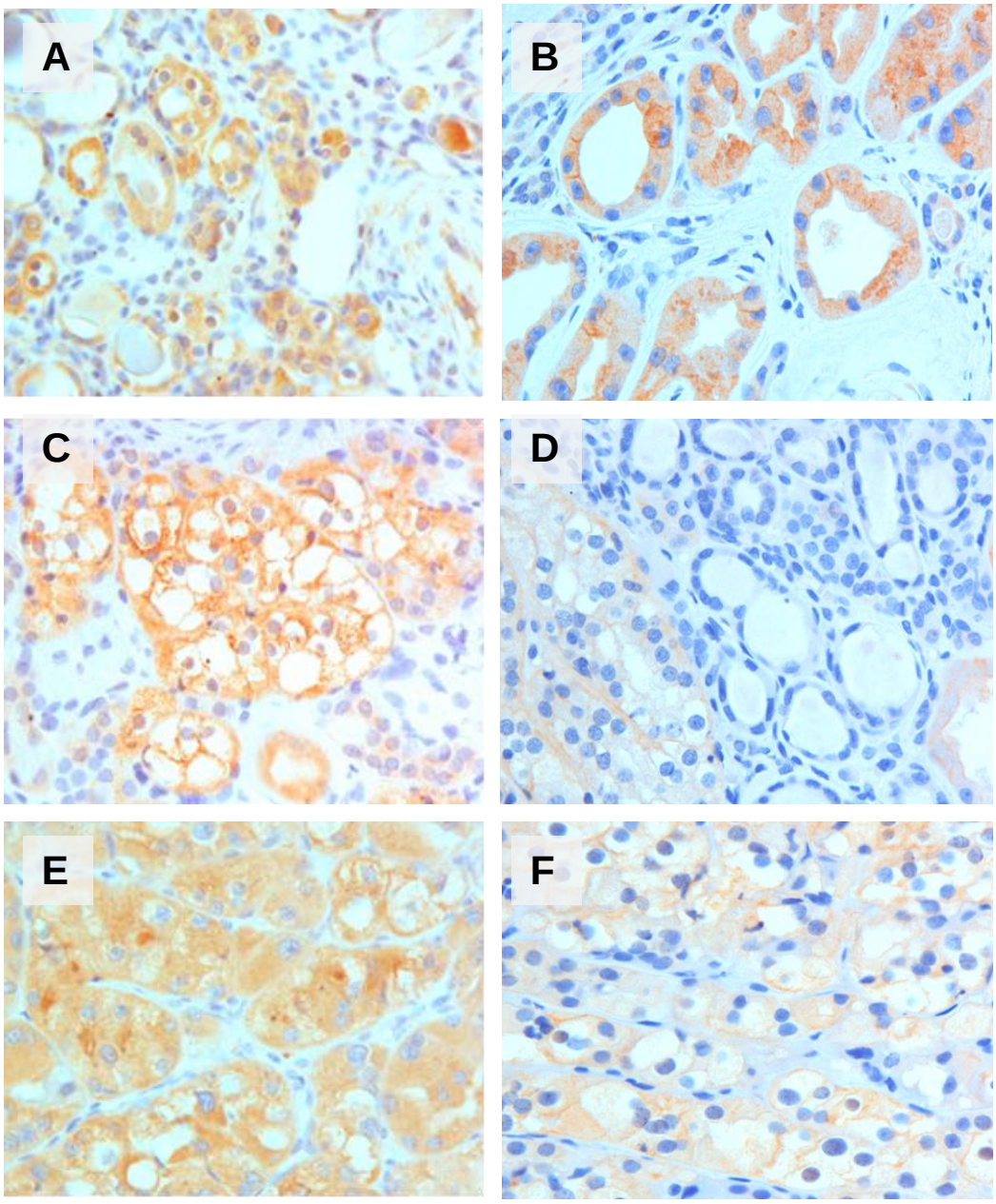

Figure 24. Expression of *CXCL8* (on the left) and its receptor *CXCR2* (on the right) in ESRD kidneys (A and B), chromophobe-like precursor lesions (C and D) and ACRD-associated tumours (E and F).

Expression of acute phase proteins SAA1 and LBP. *SAA1* was also identified by the SAM analysis as one of the genes overexpressed in ESRD/ACRD kidneys when compared to normal adult kidneys. As acute phase response genes may be also important transducer of inflammatory signals in chronic kidney disease as well, we have analysed *SAA1* for expression and cellular localization by

immunohistochemistry. We have learned from gene expression analysis of conventional RCC that lipopolysacchride binding protein (*LBP*) is expressed in invasive tumours, therefore, we have included the *LBP* in this study. Examples of immunohistochemical staining are shown in Figure 25.

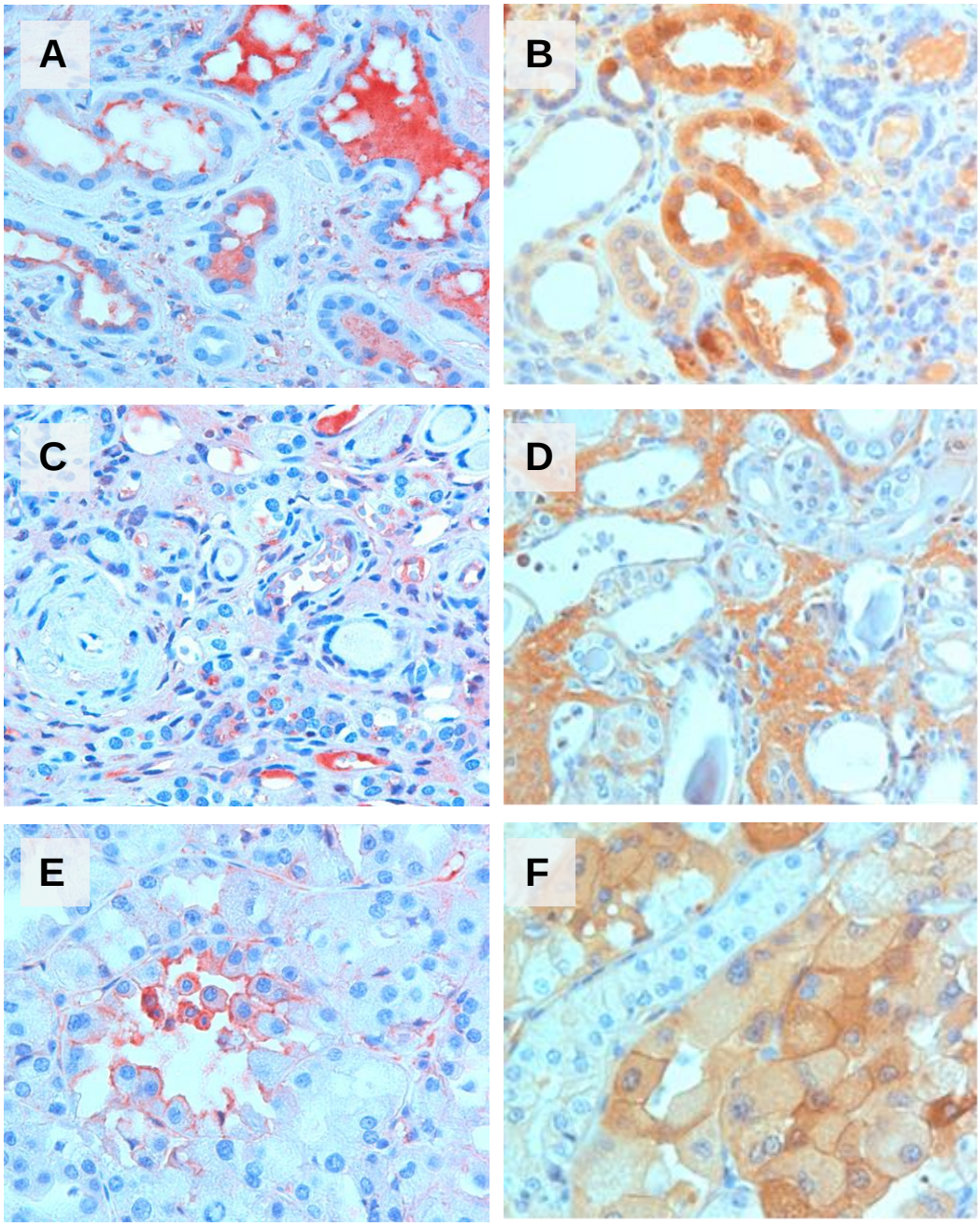

Figure 25. Expression of *SAA1* (on the left) and LBP (on the right) in ESRD kidneys (A-D) and ACRD-associated tumours (E and F).

Acute phase responsive proteins *SAA1* and *LBP* were strongly expressed in the vast majority of small or dilated tubular cells of ESRD/ACRD kidneys and also weak expression was seen in fibrotic and inflammatory stroma (Figure 25A and B). Some of the dilated tubuli were filled with *SAA1* positive fluid. The *LBP* protein was highly expressed in the fibrotic stroma of ESRD kidney, whereas the *SAA1* expression was less intensive in stromal areas (Figure 25C and D). A weak cytoplasmic reaction with attenuated cell membrane *SAA1* staining was seen in several ESRD/ACRD associated tumours (Figure 25E). Conventional RCCs as well as chromophobe-like carcinomas developed in ESRD/ACRD kidneys revealed moderate to strong *LBP* staining (Figure 25F). The latter finding corresponds to that we have obtained by analysis of conventional RCCs of the general population.

3.9.2. Group 2: Altered cytokeratin assembly

Single layered epithelial cells express normally a pair of keratin type I and II such as *KRT8* and *KRT18*, which form heterodimer. The functional analysis of specifically expressed genes indicated, that proliferating cells in ESRD/ACRD kidneys shift their keratin profile by expressing *KRT7, KRT19* and *KRT23*. We have analysed the expression of *KRT7* in ESRD/ACRD kidneys and tumours developed in kidney of ESRD/ACRD patients by immunohistochemistry. In normal kidneys, *KRT7* protein was detected in cells of the collecting duct, probably in principal cells and in thin ascending loop of Henle (Figure 26A).

We found a diffuse *KRT7* staining in nearly all areas of ESRD/ACRD kidneys, in small atrophic as well as in dilated tubules lined with flat or cuboidal or large columnar epithelial cells (Figure 26B). There was a strong immunostaining in dilated tubulus showing papillary growth within the lumen (Figure 26C). Papillary RCT developed in ESRD/ACRD kidneys showed diffuse positivity with *KRT7* antibody (Figure 26D). Of interest, membrane attenuated positive staining was seen in each small chromophobe-like precursor lesion in kidneys 173R and 173L (Figure 26E). As known from studies on chromophobe RCCs of the general population, ESRD/ACRD associated chromophobe-like RCC showed also strong membrane positivity (Figure 26F).

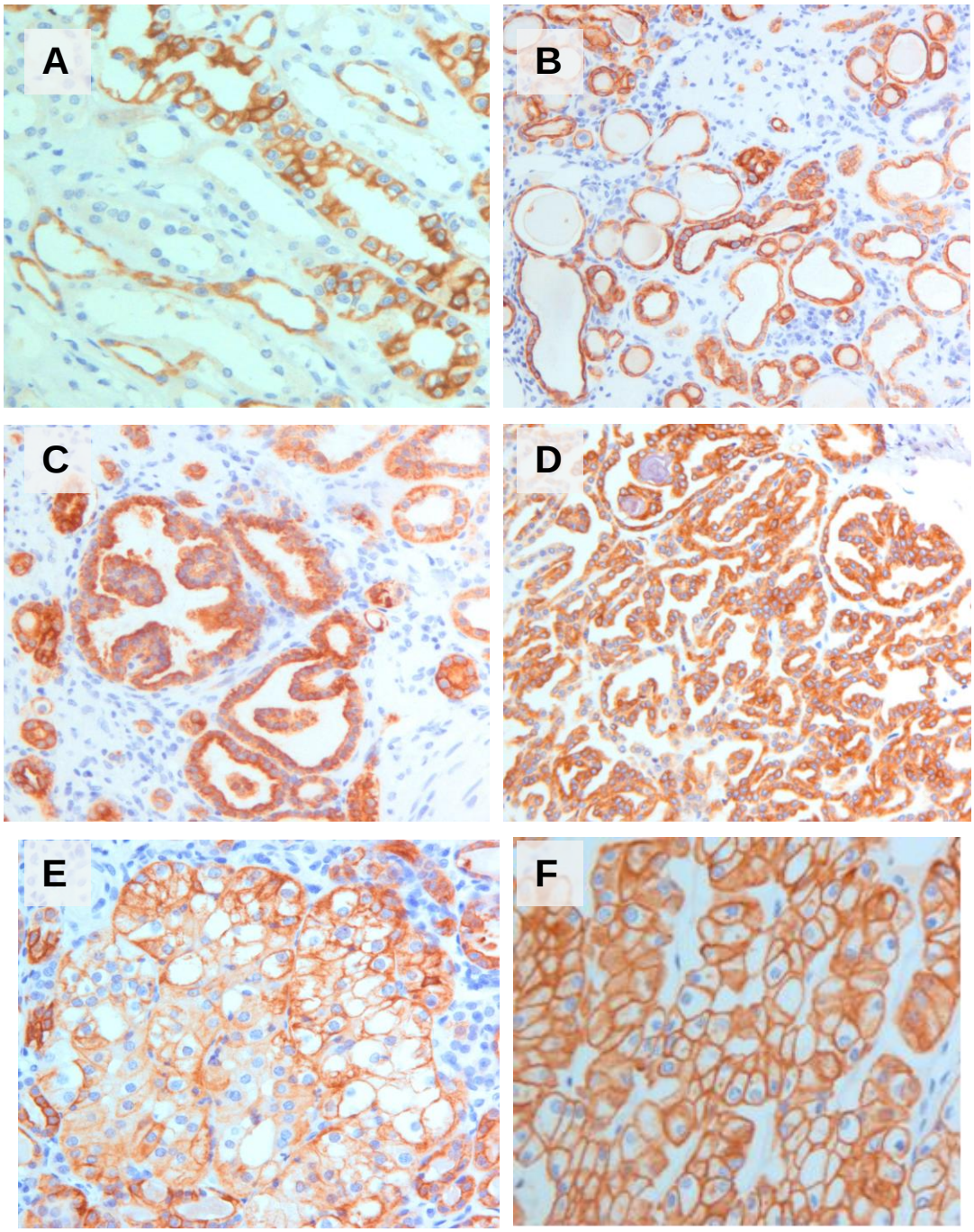

Figure 26. Positive immunohistology with *KRT7* antibody in normal kidney (A), ESRD kidney (B), papillary precursor lesion (C), papillary RCT (D), chromophobe-like precursor lesion (E) and chromophobe RCC (F).

We have analysed another member of the group of keratins overexpressed in ESRD/ACRD kidneys. *KRT19* is expressed in normal kidneys, similar to *KRT7*, in collecting duct and thin ascending loop of Henle (Figure 27A). There was a strong cytoplasmic expression in principal cells of the collecting duct. As with the *KRT7*

staining, diffuse positivity was detected in the overwhelming majority of small atrophic, normal looking or dilated tubules in ESRD/ACRD kidneys (Figure 27B). All cells of tubulary or papillary growing tumours exhibited a strong *KRT19* positive immunostaining (Figure 27C). In some ESRD/ACRD associated tumours with papillary growth pattern several tumour cells were negative for *KRT19* whereas other showed a positive staining. This type of tumour displayed broad papillary stalk with strong inflammation (Figure 27D).

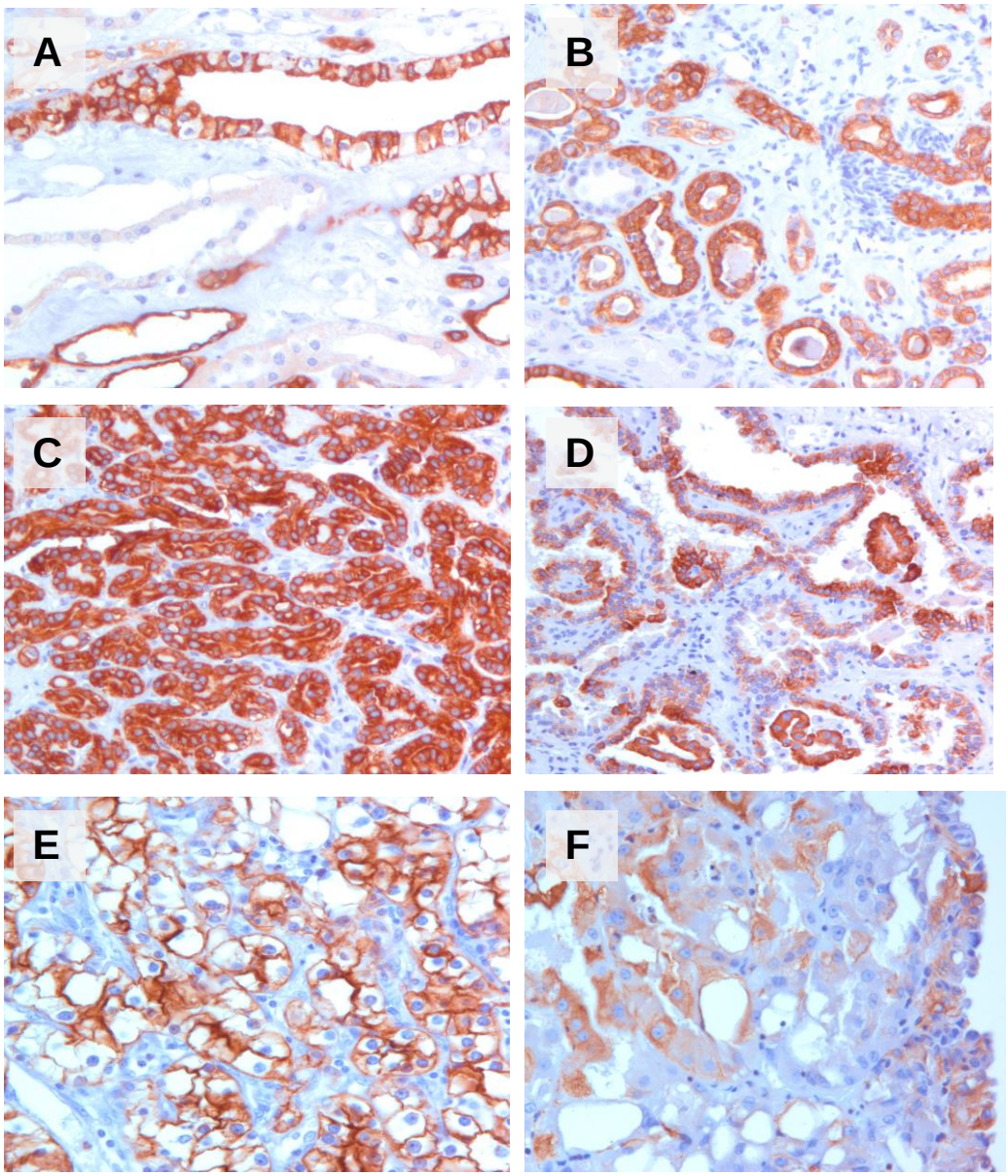

Figure 27. *KRT19* expression in normal kidney (A), ESRD/ACRD kidney (B), papillary RCTs (C and D), conventional RCC (E) and ACRD associated eosinophilic tumour (F).

Conventional RCCs were consequently negativ for *KRT7*, but showed scattered positivity for *KRT19* (Figure 27E). The ACRD associate papillary eosinophilic renal cell tumour with vacuolized cytoplasm showed focal positive immunostaining with the *KRT19* antibody (Figure 27F). We have analysed the expression of *KRT8* and *KRT18* in ESRD/ACRD kidneys and found only scattered positivity at less intensity as it was seen by *KRT7* and *KRT19* staining (not shown).

4. DISCUSSION

4.1. Are toxic effects responsible for increased risk of tumour?

Mutation of mtDNA. If toxic effects in the uremic status or during maintenance dialysis would lead to substantial DNA damage, analysis of the mitochondrial DNA in ESKD tumours would be highly informative about the severity of such alterations. We found 9 somatic nucleotide alterations in 7 of the 9 RCTs arising in kidneys of patients with ESRD/ACRD. Other studies have demonstrated somatic mtDNA mutations in 23-70% of several types of cancer (68). Most of the somatic nucleotide substitutions in tumour cells occurred in the non-coding D-loop region, in the 16S and 12S ribosomal RNA and in the *MTND4* polypeptide coding region. The D-loop region is highly polymorphic and contains hypervariable repeat units. Corresponding to this feature, the sequence variations in normal cells as well as the somatic nucleotide changes in tumour cells are clustered in the non-coding D-loop region (69). In our material 45 % of the sequence variants and of somatic mutations occurred in this region which makes up less than one sixteenth of the mitochondrial genome.

The mitochondria generate a high level of reactive oxydative species (ROS), which in concert with the low level of mtDNA repair efficiency result in a high rate of mtDNA mutations. Most somatic mutations described in the mtDNA are nucleotide transitions which correspond to ROS induced nucleotide changes (70). In several types of tumours such as colon, thyroid, ovarian and pancreas cancers G to A or T to C transitions were detected (68). In our series, 5 of the 6 somatic nucleotide substitutions were purine change four times G to A, one time A to G. Most of the somatic mtDNA mutations are homoplasmic suggesting a selective replication advantage of mutant mitochondrial genome. It was shown by fusion of colon cancer cell lines that mutant mitochondria can rapidly replace the mitochondria of recipient cells (71). We suggest that the somatic nucleotide changes in ESRD tumours occur at a very early stage of tumourigenesis, probably in progenitor cells and are selected during tumour progression as a homoplasmic mutation.

Our present study showed that the mutational rate of the mtDNA in ESRD tumours is higher than found in other types of tumours (68, 69). This may correspond to the increased level of ROS in renal parenchymal cells in ESRD/ACRD. Chronic renal diseases lead to a profound loss of parenchymal cells. Interestingly, an increased rate of proliferation has been found among cells of atrophic tubuli in ESRD kidneys (14). The cystic remodeling in ACRD is also characterized by a high rate of cell proliferation. When cells are activated by distinct stimuli, they produce ROS which in turn stimulate other cellular signalling pathways indicating that ROS may act as a second messenger (72). There is a cross talk between the cellular redox status and signalling pathways which may lead to programmed cell death or cell proliferation, both necessary for cystic remodeling processes. It is likely, that endogenic or exogenic toxic effects through increased levels of ROS promote a cell proliferation and in this complex way contribute to the development of tumours which have a high rate of ROS specific mtDNA mutations.

Genomic instability, mutation of the *VHL* gene. An increased chromosomal instability in peripheral blood lymphocytes and descreased efficiency of nuclear DNA repair has been found in uremic patients (40-43). The tumour suppressor gene p53 and the *FRA3B/FHIT* region are the target of many environmental toxic-mutagenic agents (73). However, no mutation of p53 or alteration of *FHIT* gene was seen in tumors arising in ESRD (33, 74). It is likely, that toxic or mutagenic effects do not alter the integrity of nuclear encoded genes.

Although, only few tumours from ESRD/ARCD cases have been subjected to mutation analysis of the *VHL* gene, the high frequency (83%) against those of observed in conventional RCCs in the general population (55%) may suggest a causal association of uremic- toxic status and mutation of the *VHL* gene. The increased level of ROS and hypoxemic microenvironment in ESRD/ARCD may be also responsible for the higher rate of mutation and the increased proliferation of cells may fix the mutations in the starting population of tumorigenic cells.

4.2. Recalling Virchows hypothesis: the inflammatory microenvironment

Our systematic analysis of gene expression in ESRD/ACRD kidneys identified a functional group of signature genes belonging to the chemokine family. Structurally

related members of the CXC subfamily, such as *CXCL1, CXCL3, CXCL5, CXCL6* and *CXCL8* are specifically expressed in ESRD/ACRD. These chemokines compose a cell-surface signalling assembly with *IL8* receptors *CXCR1 (IL8RA)* and *CXCR2 (IL8RB),* mediating growth-stimulatory, angiogenic or chemotactic activity on different cells types through a G-protein activated second messenger system (75). Activation of the *CXCR2* receptor might trigger neoplastic cell transformation (76). During the analysis of autocrine/paracrine role of *CXCL8* in a melanoma model the inhibition of proliferation and invasion of tumour cells has been demonstrated by neutralizing antibodies to *CXCR1* and *CXCR2* (77). The increased expression of the *CXCL8* has a critical role in tumour cell proliferation (78). The *CCL20, IL6* and *CSF2* have also stimulatory effects on growth or differentiation (79). The gene expression analysis presented here indicates a strong inflammatory microenvironment in ESRD/ACRD kidneys characterized by the expression of chemokines and cytokines and their downstream targets. Besides the chemokines a network of signalling molecules including growth factors, transcription factors and other regulatory genes are expressed in ESRD/ACRD kidneys.

Our findings recall Virchow's observation that cancers occur preferentially at sites of chronic inflammation (80). Inflammation and tumorigenesis are complex molecular processes underlying many driving forces. The finding that several genes are expressed exclusively in ESRD/ACRD and associated tumors also suggests that the inflammatory microenvironment in ESRD/ACRD can be connected to tumor development. This observation seems to improve our hypothesis on the role of specific molecular microenvironment in the development of unusual types of tumors in ESRD/ACRD, which replaces the specific genomic alterations occurring in RCTs in the general population (39).

Changes in the microenvironment activate the host immune system including the acute phase response and promote tumour growth and invasion (81). On the other hand cancer cells may shape their own microenvironment by de novo production of inflammatory mediators and acute phase proteins (82, 83). In ESRD/ACRD kidneys and associated tumours both acute phase response proteins, *SAA1* and *LBP* are expressed. *LBP* catalises a signal via a CD14-enhanced mechanism to a receptor complex including TLR-4 leading to the release of pro-inflammatory cytokines such as *IL-6* which in turn enhance *LBP* synthesis (84, 85). *TLR4* can also recognize endogenous ligands such as heat shock proteins, extra cellular matrix components

including fibronectin and heparin sulphate in response of tissue injury (86). Stimulation of *TLR4* by the *LBP-CD14* complex promotes via *MyD88* invasion through *NF-kB*-dependent up regulation of matrix metalloproteinase-2 and beta-integrin (87). Dysfunctional immunity within tumour microenvironment promotes its progression by mediating proliferative and survival signalling and promoting angiogenesis and metastasis (75, 76).

The inflammatory microenvironment in ESRD/ACRD kidney formed by stromal and infiltrating immune cells contains several factors that can promote tumorigenesis. In the chronic inflammatory process not only the above mentioned genes but also cytokines such as *TNF-alpha* and *IL6* may play crucial role. Both *TNF-alpha* and *IL6* induce free radicals, which can cause DNA damage and potentially mutations which then can lead to tumour development. Moreover, *TNF-alpha* and *IL-6* can sinergistically trigger the *TGF-beta* signalling pathway and thus promoting epithelium to mesenchyme transition and tumour invasiveness.

4.3. Increased plasticity of kidney cells during remodelling

Many types of intermediate filaments contribute towards cytoarchitecture and modulate the cellular responses to chemical stress, pro-apoptotic and other signals (88). The keratin intermediate filament assembly obligatory begins with the formation of type I and type II heterodimers (89). This requirement underlies the pairwise transcriptional regulation of keratin genes. Individual pairs of keratins are regulated in a tissue-type and differentiation-specific manner. For example, wound-proximal cells suspend their normal functions as they undergo the changes necessary to invade and repair the injured site. The keratinocytes at the site of injury suspend their programm of terminal differentiation and become activated as seen mainly through their much increased size, partial loss of cell adhesion and cytoskeletal reorganisation. This homeostatic response features major alterations in keratin gene expression. Recent studies shed light on how this structural support is modulated to meet the changing needs of cells, and reveal a novel role whereby intermediate filaments influence cell growth and death through dynamic interactions with non-structural proteins.

While highly specialized parenchymatous epithelial cells in their normal state, such as proximal tubular cells of the kidney, express only *KRT8* and *KRT18*, this

may change dramatically in reactive conditions. Upon various types of injury such as inflammation or atrophy these cells may additionally switch on *KRT7* and *KRT19*, sometimes also *KRT17* and thus express four or five instead of two keratins (90). This increased keratin expression appears to parallel the reduction in degree of differentiation. Thus, the keratin pattern of a given epithelial tissue may be modulated to some extent in the course of reactive changes, frequently resulting in higher complexity of keratin composition.

KRT19 has been described as a putative marker of epidermal stem cells (91). The expression level of *KRT19* shows a good correlation with the invasive growth and metastatic potential of liver and lung cancer and (92, 93). Serum levels of *CYFRA* 21-1, a *KRT19* fragment, have been used as a tumour marker in variety cancers such as NSCLC, breast, ovarian, liver and bladder cancer to detect tumour cell dissemination and ocurrance of metastasis (94).

By immunohistochemistry *KRT19* is expressed in normal kidney in distal tubular system extending through the entire thickness of the renal lobe but concentrated to the papillary tip. Higher magnification revealed that *KRT19* is expressed in the principal cells but not in the intercalated cells of the collecting duct. Our finding that *KRT7* especially *KRT19* is expressed in nearly all tubular structures in ESRD/ACRD kidneys can not be interpreted as an exclusive proliferation of principal cells of collecting duct but rather reflect the shift of keratin pattern of all types of tubular cells from *KRT8* and *KRT18* to *KRT 7* and *KRT19*.

The three components of the laminin332, e.g. *LAMA3*, *LAMB3* and *LAMC2* are over expressed in ESRD/ACRD kidneys. Laminins play an important role in the formation and function of the basement membrane. By interacting with other extracellular matrix components laminin332 mediates the attachment and migration and in this way the organization of cells in embryonal development of kidney and later during regeneration, tumorigenesis and metastasis (95, 96). Proliferation and migration of cells is necessary for reorganising the normal structure in end stage kidneys and in development of ESRD/ACRD associated tumours.

Several other genes selected by Affymetrix array and RT-PCR, which are overexpressed in ESRD/ACRD kidneys play a seminal role in remodeling and tumour development. For example, the protein encoded by *DCBLD2* (ESDN, endothelial and smooth muscle cell-derived neuropilin-like protein) modulates

vascular smooth muscle cell growth and is a marker of vascular remodeling (97, 98).

In summary, cells of the nephron in chronic renal disease gradually loss their normal function and suspend their program of terminal differentiation. Our findings indicate that tubular cells shift their keratin expression profile to form new cytoskeletal proteins resulting in altered shape and increased plasticity necessary for the remodeling process and tumour development.

4.4. *VDUP1/TXNIP*, tissue remodelling and increased risk of tumour

The interaction of *SCEL* with *VDUP1/TXNIP* (Vitamin D-up regulated protein 1) and the low serum level of $1\alpha,25(OH)_2D_3$ in patients with end stage renal disease promted us to analyse the *VDUP1/TXNIP* expression in a panel of samples including ESRD/ACRD kidneys. We found a strong downregulation of *VDUP1/TXNIP* in all ESRD kidneys in comparison to normal kidneys and distinct types of renal tumours. The expression of *CYP27B1* (1α-hydroxylase) was also decreased in ESRD samples against normal kidney samples. Increasing number of data suggest that *VDUP1/TXNIP* control the cell proliferation and possible the cell migration in tumour cells as well. Presumably, the low level of $1\alpha,25(OH)_2D_3$ in patients with end stage disease results from the decreased *CYP27B1* activity which in turn is indirectly associated with the lack of expression or low expression of *VDUP1/TXNIP* in ESRD kidneys.

The *VDUP1/TXNIP* which is expressed under normal conditions in several tissues, is a multifunctional protein involved in maintaining the cellular homeostasis. The low level of *VDUP1* and suspended interaction with the *SCEL* may contribute to the remodeling process, intensive proliferation of distal convoluted tubuli and high frequency of papillary RCTs in ESRD/ACRD kidneys. In addition to the elevated risk for RCT, ESRD patients show, in general, an increased risk for cancer involving not all but a number of organs (99, 100).

In summary, the observation that most patients with end stage kidneys have a decreased serum level of $1\alpha,25(OH)_2D_3$, a decreased expression level of *CYP27B1*, a substantially decreased expression of *VDUP1/TXNIP* indicate their involvement in extensive remodelling process occurring in ESRD/ARCD and possible, in the high frequency of RCT development.

5. CONCLUSIONS

Our study provides first time evidence that:

1. ***Remodeling of kidney parenchyma in ESRD/ACRD is associated with a unique gene expression signature. The specific inflammatory microenvironment, altered plasticity and proliferation rate of cells may be responsible for the structural changes in non-functioning kidneys and for the high frequency of development of RCT with unique pheno- and genotype.***

2. ***The continous expression of inflammatory cytokines yielding high level of free radicals may cause mitochondrial and genomic DNA damage and mutations which can lead to tumour development.***

3. ***Decreased expression of the multifunctional protein VDUP1/TXNIP in kidneys and other organs of patients with end stage renal disease and its suspended interaction with several molecular pathways may lead to impaired cellular homeostasis and trigger cell proliferation and tumour development.***

To characterize the unusual morphology of kidneys in ESRD/ACRD, Heptinstall applied the term “trans-Stygian pathology” referring to life beyond the mythical river (8). Our study indicates that the long survival of patients with chronic renal disease allows the kidneys to enter a "new molecular life" different from the previous one. Taking into account that an increasing number of patients are being alive "beyond the Styx" due to improved RRT and that an increasing number of these patients may develop cancer, the signaling pathways instrumental in the biology of ESRD/ACRD and related tumors merits further investigation.

6. REFERENCES

1. U.S. Renal Data System (2013) USRDS 2013. Annual Data Report: Atlas of End-Stage Renal Disease in the United States, National Institutes of Health, National Institute of Diabetes and Digestive and Kidney Diseases, Bethesda, MD.
2. Kramer A, Stel VS, Zoccali C, et al An update on renal replacement therapy in Europe: ERA-EDTA Registry data from 1997 to 2006. Nephrol Dial Transplant 2009;24:3557-3566.
3. Bommer J. Prevalence and socio-economic aspects of chronic kidney disease. Nephrol Dial Transplant. 2002;Suppl. 11:8-12.
4. Levey AS, Coresh J, Balk E, et al. National Kidney Foundation. National Kidney Foundation practice guidelines for chronic kidney disease: evaluation, classification, and stratification. Ann Intern Med. 2003;139:137-147.
5. Grassmann A, Gioberge S, Moeller S, Brown G. End-stage renal disease: global demographics in 2005 and observed trends. Artif Organs 2006;30:895-897.
6. Van Dijk PC, Jager KJ, Stengel B et al. Renal replacement therapy for diabetic end-stage renal disease: Data from 10 registries in Europe (1991-2000). Kidney Int 2005;67:1489-1499.
7. Zhang QL, Rothenbacher D. Prevalence of chronic kidney disease in population-based studies: systematic review. BMC Public Health 2008;8:117.
8. Heptinstall RH. Pathology of end-stage kidney disease. Am J Med 1968; 44:656-663.
9. Dunnill MS, Millard PR, Oliver D. Acquired cystic disease of the kidneys: a hazard of long-term intermittent maintenance haemodialysis. J Clin Pathol 1977;30:868-877.
10. McManus JF, Hughson MD, Fitts CT, Williams AV. Studies on "end-stage" kidneys. I. Nodule formation in intrarenal arteries and arterioles. Lab Invest 1977;37:339-349.
11. McManus JF, Hughson MD. New therapies and new pathologies: end-stage--dialysis kidneys. Arch Pathol Lab Med 1979;103:53-57.

12. Hughson MD, Hennigar GR, McManus JF. Atypical cysts, acquired renal cystic disease, and renal cell tumors in end stage dialysis kidneys. Lab Invest 1980;42:475-480.
13. McManus JF, Hughson MD, Hennigar GR et al. Dialysis enhances renal epithelial proliferations. Arch Pathol Lab Med 1980;104:192-195
14. Nadasdy T, Laszik Z, Blick KE, Johnson DL, Silva FG. Tubular atrophy in the end-stage kidney: a lectin and immunohistochemical study. Hum Pathol 1994; 25:22-28.
15. Grantham JJ. Acquired cystic kidney disease. Kidney Int 1991;40:143-152.
16. Levine E, Slusher SL, Grantham JJ, Wetzel LH. Natural history of acquired renal cystic disease in dialysis patients: a prospective longitudinal CT study. AJR Am J Roentgenol 1991;156:501-506.
17. Choyke PL. Acquired cystic kidney disease. Eur Radiol. 2000;10:1716-1721.
18. Matson MA, Cohen EP. Acquired cystic kidney disease: occurrence, prevalence, and renal cancers. Medicine (Baltimore) 1990;69:217-226.
19. Truong LD, Choi YJ, Shen SS et al. Renal cystic neoplasms and renal neoplasms associated with cystic renal diseases: pathogenetic and molecular links. Adv Anat Pathol 2003;10:135-159.
20. Grantham JJ, Levine E. Acquired cystic disease: replacing one kidney disease with another. Kidney Int 1985; 8:99-105.
21. Deck MA, Verani R, Silva FG, Davis LD, Cohen AH. Histogenesis of renal cysts in end-stage renal disease (acquired cystic kidney disease): an immunhistochemical and lectin study. Surg Pathol 1988;1:391-406.
22. Ishikawa I. Renal cell carcinomas in patients on long-term hemodialysis. Contrib Nephrol 1999;128:28-44.
23. Levine E, Grantham JJ, Slusher SL, Greathouse JL, Krohn BP. CT of acquired cystic kidney disease and renal tumors in long-term dialysis patients. AJR Am J Roentgenol 1984;142:125-131.
24. Hughson MD, Buchwald D, Fox M. Renal neoplasia and acquired cystic disease in patients receiving long-term dialysis. Arch Pathol Lab Med 1986;110:592-601.
25. Butler AM, Olshan AF, Kshirsagar AV et al. Cancer incidence among US Medicare ESRD patients receiving haemodialysis, 1996-2009. Am J Kidney Dis. 2015;65:763-772.

26. Gulanikar AC, Daily PP, Kilambi NK, Hamrick-Turner JE, Butkus DE. Prospective pretransplant ultrasound screening in 206 patients for acquired renal cysts and renal cell carcinoma. Transplantation 1998;66:1669-1672.
27. Moudouni SM, Lakmichi A, Tligui M et al. Renal cell carcinoma of native kidney in renal transplant recipients. BJU Int 2006;98:298-302.
28. Denton MD, Magee CC, Ovuworie C et al. Prevalence of renal cell carcinoma in patients with ESRD pre-transplantation: a pathologic analysis. Kidney Int 2002;61:2201-2209.
29. Kojima Y, Takahara S, Miyake O, Nonomura N, Morimoto A, Mori H. Renal cell carcinoma in dialysis patients: a single center experience. Int J Urol 2006;13:1045-1048.
30. Kovacs G. Molecular differential pathology of renal cell tumours. Histopathology 1993;22:1-8.
31. Kovacs G, Akhtar M, Beckwith BJ et al. The Heidelberg classification of renal cell tumours. J Pathol 1997;183:131-133.
32. Ishikawa I, Kovacs G. High incidence of papillary renal cell tumors in patients on chronic haemodialysis. Histopathology 1993;22:135-139.
33. Chudek J, Herbers J, Wilhelm M et al. The genetics and morphology of renal cell tumors in end-stage renal failure may differ from those occurring in the general population. J Am Soc Nephrol 1998;9:1045-1051.
34. Tickoo SK, dePeralta-Venturina MN, Harik LR et al. Spectrum of epithelial neoplasms in end-stage renal disease: an experience from 66 tumor-bearing kidneys with emphasis on histologic patterns distinct from those in sporadic adult renal neoplasia. Am J Surg Pathol 2006;30:141-153.
35. Pan CC, Chen YJ, Chang LC, Chang YH, Ho DM. Immunohistochemical and molecular genetic profiling of acquired cystic disease-associated renal cell carcinoma. Histopathology 2009;55:145-153.
36. Kuntz E, Yusenko MV, Nagy A, Kovacs G. Oligoarray-CGH of renal cell tumors developed in patients with acquired cystic renal disease. Hum Pathol 2011;41:1345-1349.
37. Inoue T, Matsuura K, Yoshimoto T et al. Genomic profiling of renal cell carcinoma in patients with end-stage renal disease. Cancer Sci 2012;103:569-576.

38. Sule N, Yakupoglu U, Shen SS et al. Calcium oxalate deposition in renal cell carcinoma associated with acquired cystic kidney disease: a comprehensive study. Am J Surg Pathol 2005;29:443-451.
39. Kovacs G. High frequency of papillary renal-cell tumours in end-stage kidneys--is there a molecular genetic explanation? Nephrol Dial Transplant 1995;10:593-596.
40. Cengiz K, Block AW, Hossfeld DK, Anthone R, Anthone S, Sandberg AA. Sister chromatide exchange and chromosome abnormalities in uremic patients. Cancer Genet Cytogenet 1988;36:55-67.
41. Stopper H, Boullay F, Heidland A, Vienken J, Bahner U. Comet-assay analysis identifies genomic damage in lymphocytes of uremic patients. Am J Kidney Dis 2001;38:296-301.
42. Buemi M, Floccari F, Costa C et al. Dialysis-related genotoxicity: sister chromatid exchanges and DNA lesions in T and B lymphocytes of uremic patients. Genomic damage in patients on hemodiafiltration. Blood Purif 2006;24:569-574.
43. Malachi T, Zevin D, Gafter U, Chagnac A, Slor H, Levi J. DNA repair and recovery of RNA synthesis in uremic patients. Kidney Int 1993;44:385-389.
44. Lim PS, Ma YS, Cheng YM et al. Mitochondrial DNA mutations and oxidative damage in skeletal muscle of patients with chronic uremia. J Biomed Sci 2002;9:549-560.
45. Raj DS, Boivin MA, Dominic EA et al. Haemodialysis induces mitochondrial dysfunction and apoptosis. Eur J Clin Invest 2007;37:971-977.
46. Rao M, Li L, Demello C et al. HEMO Study Group. Mitochondrial DNA injury and mortality in hemodialysis patients. J Am Soc Nephrol. 2009;20:189-196.
47. Liu CS, Ko LY, Lim PS, Kao SH, Wei YH. Biomarkers of DNA damage in patients with end-stage renal disease: mitochondrial DNA mutation in hair follicles. Nephrol Dial Transplant 2001;16:561-565.
48. Rossato LB, Nunes AC, Pereira ML et al. Prevalence of 4977bp deletion in mitochondrial DNA from patients with chronic kidney disease receiving conservative treatment or hemodialysis in southern Brazil. Ren Fail 2008;30:9-14.

49. Birch-Machin MA. The role of mitochondria in ageing and carcinogenesis. Clin Exp Dermatol 2006;31:548-552.
50. Wei YH, Lee HC. Oxidative stress, mitochondrial DNA mutation, and impairment of antioxidant enzymes in aging. Exp Biol Med 2002;227:671-682.
51. Bertram C, Hass R. Cellular responses to reactive oxygen species-induced DNA damage and aging. Biol Chem 2008;389:211-220.
52. Zuin A, Gabrielli N, Calvo IA et al. Mitochondrial dysfunction increases oxidative stress and decreases chronological life span in fission yeast. PLoS One 2008;3:e2842.
53. Torrence RJ, Elbers JD, Seline P, Clayman RV. The effect of renal cyst fluid from patients with aquired cystic disease of the kidneys (ACDK) upon the growth of benign and malignant human renal cells. J Urol 1988;139:211A.
54. Klotz LH, Kulkarni C, Mills G. End-stage renal disease serum contains a specific renal cell growth factor. J Urol 1991;145:156-160.
55. Moskowith DW, Bonar SL, Marcus MD, Clayman RV, Avner EC. Epidermal growth factor (EGF) content of human and mouse (CPK) renal cysts. Am J Kidney Dis 1989;14:435-436.
56. Mangoo-Karim R, Uchic ME, Grant M et al. Renal epithelial fluid secretion and cyst growth: the role of cyclic AMP. FASEB J 1989;3:2629-2632.
57. Konda R, Sato H, Hatafuku F, Nozawa T, Ioritani N, Fujioka T. Expression of hepatocyte growth factor and its receptor c-met in acquired renal cystic disease associated with renal cell carcinoma. J Urol 2004;171:2166-2170.
58. Taide M, Kanda S, Eguchi J, Igawa T, Kanetake H, Saito Y. A study of growth factors in human renal cysts with or without renal cell carcinoma. Clin Chim Acta 1993;217:199-203.
59. Konda R, Sugimura J, Sohma F, Katagiri T, Nakamura Y, Fujioka T. Over expression of hypoxia-inducible protein 2, hypoxia-inducible factor 1a and nuclear factor kB is putatively involved in acquired renal cyst formation and subsequent tumor transformation in patients with end stage renal failure. J Urol 2008;180:481-485.
60. Herrera GA. C-erbB-2 amplification in cystic renal disease. Kidney Int 1991;40:509-513.

61. Oya M, Mikami S, Mizuno R, Marumo K, Mukai M, Murai M. C-jun activation in acquired cystic kidney disease and renal cell carcinoma. J Urol 2005;174:726-730.
62. Yano T, Ito F, Kobayashi K et al. Hypermethylation of the CpG island of connexin 32, a candiate tumor suppressor gene in renal cell carcinomas from hemodialysis patients. Cancer Lett. 2004;208:137-142.
63. Ito F, Nakazawa H, Ryoji O, Okuda H, Toma H. Cytokines accumulated in acquired renal cysts in long-term hemodialysis patients. Urol Int 2000;65:21-27.
64. Hammes MS, Lieske JC, Pawar S, Spargo BH, Toback FG. Calcium oxalate monohydrate crystals stimulate gene expression in renal epithelial cells. Kidney Int 1995;48:501-509.
65. Fischer J, Palmedo G, von Knobloch R et al. Duplication and overexpression of the mutant allele of the MET proto-oncogene in multiple hereditary papillary renal cell tumours. Oncogene 1998;17:733-739.
66. Fellenberg K, Hauser NC, Brors B et al. Correspondence analysis applied to microarray data. Proc Natl Acad Sci U. S. A. 2001;98:10781-10786.
67. Dennis G Jr, Sherman BT, Hosack DA et al. DAVID: Database for Annotation, Visualization, and Integrated Discovery. Genome Biol 2003;4:P3
68. Chatterjee A, Mambo E, Sidransky D. Mitochondrial DNA mutations in human cancer. Oncogene 2006;25:4663-4674.
69. Yu M. Somatic mitochondrial DNA mutations in human cancers. Adv Clin Chem 2012;57:99-138.
70. Beckman KB, Ames BN. Oxidative decay of DNA. J Biol Chem 1997;272:19633-19636.
71. Polyak K, Li Y, Zhu H et al. Somatic mutations of the mitochondrial genome in human colorectal tumours. Nature Genet 1999;20:291-293.
72. Kamata H, Hirata H. Redox regulation of cellular signalling. Cell Signal 1999;11:1-14.
73. Sozzi G, Sard L, De Gregorio L et al. Association between cigarette smoking and FHIT gene alterations in lung cancer. Cancer Res 1997;57:2121-2123.
74. Bugert P, Wilhelm M, Kovacs G. FHIT gene and the FRA3B region are not involved in the genetics of renal cell carcinomas. Genes Chrom Cancer 1997;20:9-15.

75. Balkwill FR. The chemokine system and cancer. J Pathol 2012;226:148-57.
76. Strieter RM. Chemokines: not just leukocyte chemoattractants in the promotion of cancer. Nat Immunol 2001;2:285-286.
77. Varney ML, Li A, Dave BJ, Bucana CD, Johansson SL, Singh RK. Expression of CXCR1 and CXCR2 receptors in malignant melanoma with different metastatic potential and their role in interleukin-8 (CXCL-8)-mediated modulation of metastatic phenotype. Clin Exp Metast 2003;20:723-731.
78. Sparman A, Bar-Sagi D. Ras-induced interleukin-8 expression plays a critical role in tumor growth and angiogenesis. Cancer Cell 2004;6:447-458.
79. Ning Y, Nanegold PC, Hong YK et al. Interleukin-8 is associated with proliferation, migration, angiogenesis and chemosensitivity in vitro and in vivo in colon cancer cell line models. Int J Cancer 2011;128:2038-2049.
80. Virchow R. Die krankhaften Geschwülste (Dreissig Vorlesungen, gehalten wahrend des Wintersemesters 1862-1863) Band I. August Hirschwald, Berlin, Germany
81. Balkwill F, Mantovani A. Inflammation and cancer: back to Virchow? Lancet 2001;357:539-545.
82. Allavena P, Germano G, Marchesi F, Mantovani A. Chemokines in cancer related inflammation. Exp Cell Res 2011;317:664-673.
83. Orr WS, Malkas LH, Hickey RJ, Sandoval JA. Acute Phase Proteins as Cancer Biomarkers, Acute Phase Proteins as Early Non-Specific Biomarkers of Human and Veterinary Diseases, Prof. Francisco Veas (Ed.) (2011). ISBN: 978-953-307-873-1, InTech, DOI: 10.5772/25181.
84. Faure E, Equils O, Sieling PA. Bacterial lipopolysacchride activates NF-kappaB through toll-like receptor 4 (TLR-4) in cultured human dermal endothelial cells. Differential expression of TLR-4 and TLR-2 in endothelial cells. J Biol Chem 2000;275:11058-11063.
85. Kitchens RL, Thompson PA. Modulatory effects of sCD14 and LBP on LPS-host cell interactions. J Endotoxin Res 2005;11:225-229.
86. Akira S, Takeda K. Toll-like receptor signalling. Nat Rev Immunol 2011;4:499-511

87. Harmey JH, Bucana CD, Lu W et al. Lipopolysaccharide-induced metastatic growth is associated with increased angiogenesis, vascular permeability and tumor cell invasion. Int J Cancer 2002;101:415-422.
88. Coulombe PA, Wong P. Cytoplasmic intermediate filaments revealed as dynamic and multipurpose scaffolds. Nat Cell Biol 2004;8:699-706.
89. Coulombe PA, Bernot KM. Keratins and the skin, p. 497-504. In M. D. Lane and W. Lennarz (ed.), (2004) Encyclopedia of biological chemistry. Elsevier Science, New York, N.Y.
90. Moll R, Divo M, Langbein L. The human keratins: biology and pathology. Histochem Cell Biol 2008;129:705–733.
91. Commo S, Gaillard O, Bernard BA. The human hair follicle contains two distinct K19 positive compartments in the outer root sheath: a unifying hypothesis for stem cell reservoir? Differentiation 2000;66:157-164.
92. Tang J, Zhuo H, Zhang X et al. A novel biomarker Linc00974 interacting with KRT19 promotes proliferation and metastasis in hepatocellular carcinoma. Cell Death Dis 2014;5:e1549.
93. Okamura K, Takayama K, Izumi M et al. Diagnostic value of CEA and CYFRA 21-1 tumor markers in primary lung cancer. Lung Cancer 2013;80:45-49.
94. Huang YL, Chen J, Yan W et al. Diagnostic accuracy of cytokeratin-19 fragment (CYFRA 21-1) for bladder cancer: a systematic review and meta-analysis. Tumor Biol 2015;36:3137-3145.
95. Marinkovich MP. Tumour microenvironment: laminin 332 in squamous-cell carcinoma. Nat Rev Cancer 2007;7:370-380.
96. Carpenter PM, Wang-Rodriguez J, Chan OT, Wilczinski SP. Laminin 5 expression in metaplastic breast carcinomas. Am J Surg Pathol 2008;32:345-353.
97. Guo X, Nie L, Esmailzadeh L, Zhang J, Bender JR, Sadeghi MM. Endothelial and smooth muscle-derived neuropilin-like protein regulates platelet-derived growth factor signaling in human vascular smooth muscle cells by modulating receptor ubiquitination. J Biol Chem 2009;284:29376-29382.
98. Sadeghi MM, Esmailzadeh L, Zhang J et al. ESDN is a marker of vascular remodeling and regulator of cell proliferation in graft arteriosclerosis. Am J Transplant 2007; 7: 2098-2105.

99. Butler AM, Olshan AF, Kshirsagar AV et al. Cancer incidence among US Medicare ESRD patients receiving hemodialysis, 1996-2009. Am J Kidney Dis 2015;65:763-772.
100. Lin HF, Li YH, Wang CH et al. Increased risk of cancer in chronic dialysis patients: a population-based cohort study in Taiwan. Nephrol Dial Transplant 2012;27:1585-1590.

7. PUBLICATIONS OF THE AUTHOR

Original research publications related to the thesis

Nagy A, Walter E, Zubakov D, Kovacs G. High risk of development of renal cell tumor in end stage kidney disease: the role of microenvironment. Tumor Biol 2016;37:9511-9519.

IF: 3.611 cit:0

Nagy A, Banyai D, Semjen D, Beothe T, Kovacs G. Sciellin is a marker for papillary renal cell tumours. Virchows Archiv 2015;467:695-700.

IF: 2.651 cit: 0

Kuntz E, Yusenko MV, **Nagy A,** Kovacs G. Oligoarray comparative genomic hybridization of renal cell tumors that developed in patients with acquired cystic renal disease. Hum Pathol 2010 41:1345-9.

IF:2.998 cit: 5

Chudek J, **Nagy A,** Kokot F, Podwinski A, Wiecek A, Ritz E, Kovacs G. Phosphatemia is related to chromosomal aberrations of parathyroid glands in patients with hyperparathyroidism. J Nephrol 2007;20:164-72.

IF:1.138 cit: 3

Nagy A, Wilhelm M, Kovacs G. Mutations of mtDNA in renal cell tumours arising in end-stage renal disease. J Pathol 2003;199:237-242.

IF:4.933 cit: 36

Nagy A, Chudek J, Kovacs G. Accumulation of allelic changes at chromosomes 7p, 18q, and 2 in parathyroid lesions of uremic patients. Lab Invest 2001;81:527-533.

IF:3.934 cit: 7

Berczi C, **Nagy A,** Matyus J, Balazs G, Kakuk G, Lukacs G. [Results and complications of parathyroidectomy in secondary hyperparathyroidism] Magy Seb. 2001;54:356-360. Hungarian

IF:0 cit: 0

Original publications not related to the thesis

Beothe T, **Nagy A,** Farkas L, Kovacs G. P53 mutation and LOH at chromosome 9 in urothelial carcinoma. Anticancer Res 2012;32:523-527.

IF:1.713 cit: 1

Yusenko MV, **Nagy A,** Kovacs G. Molecular analysis of germline t(3;6) and t(3;12) associated with conventional renal cell carcinomas indicates their rate-limiting role and supports the three-hit model of carcinogenesis. Cancer Genet Cytogenet 2010;201:15-23.

IF:1.551 cit: 4

Nagy A, Buzogany I, Kovacs G. Microsatellite allelotyping differentiates chromophobe renal cell carcinomas from renal oncocytomas and identifies new genetic changes. Histopathology 2004;44:542-546.

IF:2.955 cit: 32

Balint I, Muller A, **Nagy A,** Kovacs G. Cloning and characterisation of the RBCC728/TRIM36 zinc-binding protein from the tumor suppressor gene region at chromosome 5q22.3. Gene 2004;332:45-50.

IF:2.705 cit: 11

Nagy A, Zoubakov D, Stupar Z, Kovacs G. Lack of mutation of the folliculin gene in sporadic chromophobe renal cell carcinoma and renal oncocytoma. Int J Cancer 2004;109:472-475.

IF:4.416 cit: 31

Nagy A, Balint I, Kovacs G. Frequent allelic changes at chromosome 7q34 but lack of mutation of the BRAF in papillary renal cell tumors. Int J Cancer 2003;106:980-981.

IF:4.375 cit: 11

Nagy A, Wilhelm M, Sukosd F, Ljungberg B, Kovacs G. Somatic mitochondrial DNA mutations in human chromophobe renal cell carcinomas. Genes Chromosomes Cancer 2002;35:256-260.

IF:4.199 cit: 40

Összesített IF: 41.179
Citation: 180
Hirsch index: 7

Abstracts, presentations

Nagy A, Mátyus J, Kakuk Gy. Analgeticum nephropathiás betegek követése során szerzett tapasztalataink. Magyar Nephrologiai Társaság XV. Nagygyűlése, Budapest, 1998.

Chudek J, **Nagy A,** Kovács Gy. A HGF/SF és MET koexpressziója vese parenchymális sejteken végstádiumú veseelégtelenségben. Magyar Nephrologiai Társaság XVIII. Nagygyűlése, Balatonaliga, 2001.

Nagy A, Kovács Gy. Globális génexpresszió vizsgálata végstádiumú vesében. Magyar Nephrologiai Társaság XXI. Nagygyűlése, Eger, 2004.

Nagy A, Fellenberg K, Kovacs G. New life after death: a unique expression profil during remodelling of end stage kidneys. Magyar Patológusok Társaságának 2005. évi Kongresszusa, Pécs, 2005.

Nagy A, Chudek J, Kovacs G. Frequent allelic changes at chromosomes 7p, 18q and 2p in parathyroid lesions of uremic patients. Magyar Nephrologiai Társaság XVII. Nagygyűlése, Budapest, 2000.

Nagy A, Chudek J, Kovacs G. Coexpression of HGF/SF and its receptor MET in renal epithelial cells in end-stage renal disase. Magyar Patológusok Társaságának 2000. évi Kongresszusa, Eger, 2000.

Nagy A., Wilhelm M., Kovács Gy. Mitokondriális DNS mutációk urémiás betegekben kialakult vesesejt tumorokban. Magyar Nephrologiai Társaság XIX. Nagygyűlése, Siófok, 2002.

8. ACKNOWLEDGEMENT

Foremost, I would like to express my gratitude to Professor György Kakuk, the previous head of the 1st Department of Medicine and its Division of Nephrology and Professor József Balla, the current head of the Division of Nephology in the Medical University of Debrecen for their generous support making my scientific work possible abroad and helping me in respect to my stipendiums. From the great nephrological team, I am much obliged to Dr. János Mátyus who had a significant role that I could build a relationship with my later supervisor, Professor Gyula Kovacs and could realize my scholarship in Heidelberg. His collegiual friendship and encouragement means a great deal to me.

I am highly indebted and sincere thankful to my supervisor, Professor Gyula Kovacs who gave me the opportunity to establish my research work from the first steps and provided all the facilities in the former Laboratory of Molecular Oncology, Ruprecht-Karls University of Heidelberg. I have the honor to possess his tenacious support and motivation and I am grateful for appreciating my efforts. My gratitude is extended to all my former fellows in this laboratory who helped me to acquire the technical knowledge and shared me experiences.

I appreciate the possibility to complete my work in a Doctoral School leaded by Professor Gábor Kovacs L. including a program leaded by Professor István Wittmann at the University of Pécs Medical School. I am truly grateful to Dr. Tamás Beöthe from the Department of Urology, for his valuable helpfulness.

I owe sincere and deep thankfulness to my family, especially my parents and sister for doing their best and standing by me every time I needed. This thesis is dedicated to my parents constantly providing loving care for my family life as well as supporting my studies.